NAVAL POSTGRADUATE SCHOOL
Monterey, California

②

AD-A218 390

TIC
ECTE
FEB 14 1990
D
D

THESIS

DETERMINATION OF THE VELOCITY,
DENSITY, MAXIMUM FLUX AND ENTHAPLY
PROFILES FOR A VERY HIGH
TEMPERATURE ARC JET NOZZLE FLOW.

by
Robert William Kopp
June 1989

Thesis Advisor (NASA Ames):   Warren Winovich
Thesis Advisor: Prof Richard Wood

90 02 ?? ?0

REPORT DOCUMENTATION PAGE

1a Report Security Classification Unclassified	1b Restrictive Markings
2a Security Classification Authority t	3 Distribution Availability of Repor
2b Declassification/Downgrading Schedule	Approved for public release; distribution is unlimited.

4 Performing Organization Report Number(s)	5 Monitoring Organization Report Number(s)

6a Name of Performing Organization Naval Postgraduate School	6b Office Symbol 31	7a Name of Monitoring Organization Naval Postgraduate School
6c Address (city, state, and ZIP code) Monterey, CA 93943-5000		7b Address (city, state, and ZIP code) Monterey, CA 93943-5000

8a Name of Funding/Sponsoring Organization	8b Office Symbol	9 Procurement Instrument Identification Number
8c Address (city, state, and ZIP code)		10 Source of Funding Numbers

Program Element Number	Project No	Task No	Work Unit Accession No

11 Title (Include Security Classification)
DETERMINATION OF THE VELOCITY, DENSITY, MASS FLUX, AND ENTHALPY PROFILES FOR A VERY HIGH TEMPERATURE ARCJET NOZZLE FLOW

12 Personal Author(s) Kopp, Robert W.

13a Type of Report Master's Thesis	13b Time Covered From To	14 Date of Report (year, month, day) June 1989	15 Page Count 63

16 Supplementary Notation The views expressed in this thesis are those of the author and do not reflect the official policy or position of the Department of Defense or the U.S. Government.

17 Cosati Codes			18 Subject Terms (continue on reverse if necessary and identify by block number)
Field	Group	Subgroup	Arcjet flow, Hypervelocity flow, High enthalpy flow, Flow characteristics, Characteristic profile of the flow, Theses. (JAO)

19 Abstract (continue on reverse if necessary and identify by block number)

Hypervelocity flows for velocities is excess of 1.4 km/sec (Mach 5) require very high stagnation temperature to avoid liquefaction. The arc heater wind tunnel has been designed to provide such flows. The electric-arc driven wind tunnel can develop stagnation temperatures up to $13,000°K$ which will produce hypervelocity flows up to 7 km/sec (earth orbital speed). The nature of the flow, however, is such that the high temperature source flow may cause severe gradients at the nozzle exit. In order to perform aero-thermodynamic tests the characterization of the flow in the test section is required. This paper experimentally determines the stream profiles for an arcjet wind tunnel conical nozzle directly from calorimetry and pitot probe surveys. keywords:

20 Distribution/Availability of Abstract [X] unclassified/unlimited [ ] same as report [ ] DTIC users	21 Abstract Security Classification Unclassified	
22a Name of Responsible Individual Prof Richard Wood	22b Telephone (Include Area code) (408) 646-2944	22c Office Symbol 67 Wr

DD FORM 1473, 84 MAR 83 APR edition may be used until exhausted security classification of this page
All other editions are obsolete Unclassified

DETERMINATION OF THE VELOCITY, DENSITY, MASS FLUX AND ENTHALPY PROFILES FOR VERY HIGH TEMPERATURE ARC JET NOZZLE FLOW.

by

Robert William Kopp
Lieutenant Commander, United States Navy
B.S., University of South Alabama, 1976

Submitted in partial fulfillment of the requirements for
the degree of

MASTER OF SCIENCE IN AERONAUTICAL ENGINEERING

from the

NAVAL POSTGRADUATE SCHOOL
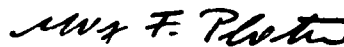June 1989

Author: _____

Robert William Kopp

Approved by: _____

Richard D. Wood, Thesis Advisor

_____

Raymond P. Shreeve, Second Reader

_____

E. RobertsWood, Chairman,
Department of Aeronautics and Astronautics

_____

Gordon E. Schacher, Dean of Science and Engineering

ii

ABSTRACT

Hypervelocity flows for velocities in excess of 1.4 km/sec (Mach 5) require very high stagnation temperature to avoid liquefaction. The arc heater wind tunnel has been designed to provide such flows. The electric-arc driven wind tunnel can develop stagnation temperatures up to 13,000°K which will produce hypervelocity flows up to 7 km/sec (earth orbital speed). The nature of the flow, however, is such that the high temperature source flow may cause severe gradients at the nozzle exit. In order to perform aero-thermodynamic tests the characterization of the flow in the test section is required. This paper experimentally determines the stream profiles for an arc jet wind tunnel conical nozzle directly from calorimetry and pitot probe surveys.

TABLE OF CONTENTS

LIST OF SYMBOLS

SYMBOLS

A	Amps
atm	Atmospheric pressure
h	Enthalpy
M	Mach number
mf	Mass flux
mmHg	Millimeters of mercury
MW	Megawatt
p	Pressure
$\dot{q}$	Heat transfer rate
R	Universal gas constant
V	Volts
V	Velocity

GREEK SYMBOLS

γ	Ratio of specific heats
ρ	Density

SUBSCRIPTS

CL	Centerline
t	Stagnation conditions
w	Wall conditions
1	Upstream of normal shock
2	Downstream of normal shock

ACKNOWLEDGMENTS

Special thanks to Warren Winovich for his recommendation to undertake this effort. Through his insight and valuable experience I have gained a partial understanding of the arcjet facilities he helped create.

Special thanks to Professor R. P. Shreeve whose outstanding teaching ability and patience have inspired me in the field of hypersonic aerodynamics.

Thanks to John Balboni who always had a encouraging attitude towards myself and my work even though it took time away from his own work.

I would most of all like to thank my wife, Janeen, whose never ending support for me and dedication to our two boys has enabled me to complete this effort and the graduate program. I shall be eternally grateful to her for this.

I. INTRODUCTION

This report is concerned with developing a procedure by which flow field characteristics of very high temperature arcjet flows may be produced directly from stream surveys of nozzles.

Hypervelocity flight in the atmosphere has previously been concerned with entry into the atmosphere and descent to the ground. This has been expanded during the last decade to include vehicles which will use the upper layers of the atmosphere to perform hypervelocity aerodynamic maneuvers and vehicles which will fly from the ground into orbit using air breathing powered lift. The design and testing of an aeroassisted orbital transfer vehicle (AOTV) and the National Aerospace Plane (NASP) will require ground based testing in order to obtain a data base for this flight regime. Such data will be used to validate 3-D, reacting real-gas, CFD codes that will be used in the design of advanced vehicles where aero-thermodynamic effects are important.

The 60-MW Shuttle Interaction Heating Facility (IHF) was designed to meet the testing requirements for development of the thermal protection system of the shuttle orbiter vehicle. Its design provided for heat transfer simulation and stagnation-region flow simulation for conditions which the shuttle orbiter would encounter. If this facility is to be used in aerodynamic testing, the arcjet flow characteristics need to be known in order to determine if they provide optimum simulation of the actual flow conditions.

In arcjet operations, extremely high temperatures are generated. For example, for the test reported here, the stagnation temperatures are of the order of 6000°K (10,800°R). Probes must be highly cooled in order to survive the environment.

1

Conventional techniques using thermocouples, for example, to determine local stream energy simply will not work because of these high temperatures. Stream tube flow-swallowing techniques can be used up to moderate temperatures, however, such enthalpy probes require sharp leading edges; and these can not be cooled in the arcjet environment. Moreover, such probes with blunt cooled leading edges yield an uncertain stream-tube capture; and resolution and accuracy both have large uncertainties. To circumvent these problems for arcjet stream surveys, a simple method has been developed that uses small diameter, cooled, hemispherical-shaped probes to measure local heat transfer and pitot pressure. It is shown in this report that these two measurements yield stream profiles to a high degree of resolution. The theoretical method derived here has been formulated into a computer code for data reduction of stream surveys. This code can be incorporated into a real-time data acquisition system and will provide on-line reduced stream profiles during the nozzle survey for immediate assessment.

PROFILE is a computer code developed to use the 60-MW IHF stream survey data for a 13-inch conical nozzle. The PROFILE code directly produces normalized velocity, density, mass flux and enthalpy profiles. The derivation of PROFILE uses the basic conservation equations and is described in Chapter IV. PROFILE uses the heat transfer and stagnation pressure data as inputs and outputs normalized values of heat transfer rates, stagnation pressure, velocity, density, mass flux and enthalpy with respect to centerline values of the flow. Characteristics of flows for other arcjet designs and other nozzles can be readily obtained using heat transfer and stagnation pressure survey data in conjunction with the PROFILE code developed here.

2

II. INTERACTION HEATING FACILITY DESCRIPTION

A schematic diagram and photograph of the IHF arcjet facility are shown in Figure 1 and 2, respectively. The major components of the facility include a constricted-arc air heater, a 150 MW power supply, two interchangeable hypersonic Mach number nozzles, a walk-in test chamber, and ancillary subsystems consisting of a steam-ejector vacuum system, cooling water system, and automated data acquisition system. The high-power capability of the arc heater (rated to 60 MW) provides for full scale subsystem tests in high enthalpy streams in both large scale stagnation flows and boundary layer flows at high Reynolds numbers.

The primary component of the facility is a constricted-arc heater 390 cm (153.3 in.) long and 8 cm (3.15 in.) in diameter shown in Figure 3. The rated airflow rate is 1.4 kg/s (3.09 lbs/s) and the rated pressure is 12 atm. Cooling water is supplied at 7000 kPa (1000 psi), which provides cooling for a maximum heating of 12 kW/cm^2 to the constrictor wall. Eight anode and cathode electrodes, each capable of conducting 1000 A, provide a maximum arc current capacity of 8000 A. Thus, the capability for continuous operation at high current and high enthalpy levels is provided.

Direct current for operating the arc heater is provided by a 150 MW D.C. power supply. Six modules make up the power supply, each consisting of a three-phase, full-wave, phase controlled silicon rectifier. One module is capable of operating up to a level of 5500 V into an arc load at current levels up to 2700 A. The six modules can be connected in any compatible series/parallel arrangement by means of remotely operated setup switches. The duty cycle for the power supply is

3

30 minutes on, 30 minutes off. A 150 MW rating is achieved for run durations of approximately 15 seconds.

The facility has two interchangeable nozzles: 1) a semielliptic, Mach number 5 nozzle with an open-jet, flat-plate test section measuring 80 X 80 cm (31.5 X 31.5 in.) for boundary-layer surface flow tests and 2) a conical, nozzle for testing large-scale stagnation flows in a free jet. The conical nozzle is constructed in 5 sections with exit diameters varying from 15.24 cm (6 in.) to 105 cm (41.4 in.). The Mach number varies with the nozzle area ratio from 3 to 7.5 depending on the exit diameter selected. Both nozzles are water cooled by internal water passages, and the throat diameters are 6.03 cm (2.37 in.). Both nozzles are designed to flow into an evacuated, walk-in test chamber that can be maintained at a pressure of less than 0.004 atm (3 mmHg), a pressure that varies with flow rate according to the pumping curve of the steam ejector system. Tests have shown that supersonic flow with 33 % blockage ratio has been attained in the conical nozzle, corresponding to a model diameter of about 60 cm (24 in.).

An on-line automated data acquisition and computing system is used to record arcjet performance and test data. The conversion from analog to digital signals is made by means of an integrating digital voltmeter, so that the signals can be processed by an on-line computer. Output consists of a real-time display of five channels that are monitored during a run, printed and reduced data, and a continuous time history data plot. [Ref. 1]

4

III. SURVEY DESCRIPTION

The design of the IHF allows for the control of two variables: 1) constrictor pressure and 2) arc current. The test conditions are uniquely determined by these two control settings only. For this survey, the test chamber pressure was maintained at a low pressure to allow the measurements to be made in a free jet. No attempt was made to control the expansion ratio into the free-jet chamber. In general, the flow was as an under-expanded free jet. This type of operation causes the free jet to spread and to operate at a slightly higher Mach number relative to the nozzle exit plane.The survey measurements close to the nozzle exit plane, then are relatively uninfluenced by the free-jet expansion process. Most of the discussion pertains to the 7.62-cm (3-inch) station to avoid the complexity of the additional expansion. Constrictor pressure was varied for several values of current in order to map the operating envelope for stagnation flows using the conical nozzle.

The probes used to obtain data consisted of a hemispherical Gardon type calorimeter and a pitot probe shown in Figures 5 and 6. The probes were 1.58 cm (0.625 in) in diameter and were mounted 20.32 cm (8.0 in) apart horizontally. The probes were mounted to a transverse mechanism that was positioned to pass horizontally through the flow. Sweep measurements were taken at 7.62 cm (3.0 in), 19.5 cm (7.7 in), 34.8 cm (13.7 in) and 52.6 cm (20.7 in) downstream of the nozzle exit.

Figure 7 shows probes, probe supports and their relationship to the nozzle during a test using a 15.24 cm (6.0 in.) exit diameter nozzle. Figure 8 shows probes entering the flow. Figure 9 shows probes approximately on centerline of

5

nozzle. All photographs were taken using only radiated light from gas behindthe normal shocks on probes and support mechanisms.

Data consisted of heat transfer rate and stagnation pressure measurements taken at 0.212 cm (0.083 in.) intervals across the flow. Typical profiles for heat transfer rate and stagnation pressure for each current setting are shown in Figure 10.

IV. DERIVATION OF DIRECT METHOD FOR PROFILES

Determining the stream profiles for an arcjet wind tunnel nozzle requires that the heat transfer rate and the stagnation pressure measurements behind a normal shock make up the only parameters on which the velocity characteristics depend. Briefly, this method is based on the fact that stagnation-point heat transfer is proportional to the product ρV^3 (approximately) while the pitot pressure is proportional to ρV^2. When these two quantities are known, a simultaneous solution gives density and velocity directly from the measurements. Once the velocity profile has been determined the profiles for enthalpy, mass flux and density can be readily found.

In the following derivation, free stream flow parameters are those found in front of the normal shock and will be designated by subscript one while subscript two will denote parameters behind the normal shock. The starting point is the momentum and continuity equations in the following form:

$$p_1 + \rho_1 V_1^2 = p_2 + \rho_2 V_2^2 \tag{1}$$

$$\rho_1 V_1 = \rho_2 V_2 \tag{2}$$

Rearranging the momentum equation and substituting into it the continuity equation gives:

$$p_2 \left(1 - \frac{1}{\frac{p_2}{p_1}} \right) = \rho_1 V_1^2 \left(1 - \frac{1}{\frac{\rho_2}{\rho_1}} \right) \tag{3}$$

Solving for p_2

$$p_2 = \rho_1 V_1^2 \left(\frac{1 - (1/(\rho_2/\rho_1))}{1 - (1/(p_2/p_1))} \right) \tag{4}$$

7

Noting that M_2 is much less than 1, that $M_2 = \varphi(\gamma, M)$ and recalling that from state 2 to stagnation state 2 is along an isentrope then:

$$p_{t_2} = p_2 \left(1 + \left(\frac{\gamma - 1}{2}\right) M_2^2\right)^{\gamma/(\gamma-1)}$$

(5)

Normalizing equation (5) with centerline values results in

$$\frac{p_{t_2}}{\left(p_{t_2}\right)_{CL}} \cong \frac{p_2}{\left(p_2\right)_{CL}}$$

(6)

Substituting equation (6) into a normalized equation (4) gives:

$$\frac{p_{t_2}}{\left(p_{t_2}\right)_{CL}} \cong \frac{\rho_1 V_1^2}{\left(\rho_1 V_1^2\right)_{CL}}$$

(7)

At this point the normalized stagnation pressure behind the shock is related to the velocity in front of the shock. The next step introduces the closed form of the Fay-Riddell [Ref 2] equation derived in Appendix A., which is a correlation for the heat transfer rate to a hemisphere; namely,

$$\dot{q} = 0.0417 \sqrt{\frac{p_{t_2}}{R}} \, (h_t - h_w) \quad \text{(Btu/sec-ft}^2\text{)}$$

(8)

where h_t is the total enthalpy of the flow and h_w is the enthalpy of the wall. The units are: h, Btu/lb$_m$; p_{t2}, atm; and R, ft. Normalizing with centerline values gives:

8

$$\frac{\dot{q}}{(\dot{q})_{CL}} = \sqrt{\frac{P_{t_2}}{\left(P_{t_2}\right)_{CL}}\left(\frac{(h_t - h_w)}{(h_t - h_w)_{CL}}\right)} \tag{9}$$

Using the following form of the energy equation

$$h_1 + \frac{V_1^2}{2} = h_2 + \frac{V_2^2}{2} = h_t \tag{10}$$

and equation (7) in equation (9) while neglecting the enthalpy of the wall compared to the total enthalpy of the flow yields:

$$\frac{\dot{q}}{(\dot{q})_{CL}} = \sqrt{\frac{\rho_1 V_1^2}{\left(\rho_1 V_1^2\right)_{CL}} \frac{(V_1^2 + 2h_1)}{(V_1^2 + 2h_1)_{CL}}} \tag{11}$$

Rearranging

$$\frac{\dot{q}}{(\dot{q})_{CL}} = \sqrt{\frac{\rho_1}{(\rho_1)_{CL}}} \left(\frac{V_1}{(V_1)_{CL}}\right)^3 \frac{\left(1 + \frac{2h_1}{V_1^2}\right)}{\left(1 + \frac{2h_1}{V_1^2}\right)_{CL}} \tag{12}$$

Since the velocity in front of the shock is supersonic the last term drops out. Changing notation to reflect only centerline and free stream gives:

9

$$\frac{\dot{q}}{(\dot{q})_{CL}} = \sqrt{\frac{\rho_1}{(\rho_1)_{CL}}} \left(\frac{V_1}{(V_1)_{CL}}\right)^3$$

(13)

Squaring equation (13) and dividing by equation (7) removes the density term and results in an equation which relates free stream velocity, stagnation pressure and heat flux.

$$\left(\frac{V}{V_{CL}}\right)^4 = \left(\frac{\dot{q}}{\dot{q}_{CL}}\right)^2 \left(\frac{p_t}{p_{t_{CL}}}\right)^{-1}$$

(14)

This equation equates the normalized velocity of the free stream to the two measured quantities behind the normal shock.

The assumption made to derive this result are simply that the flow is axisymmetric and the enthalpy of the wall is small compared with the total enthalpy of the free flow. The wall enthalpy is measured directly from cooling water and is found to be approximately 0.3 MJ/kg (134 Btu/lbm) or less than 5 % of total enthalpy.

Once the normalized velocity has been found it is used in equation (7) to find the value for the normalized density.

$$\frac{\rho}{\rho_{CL}} = \frac{p_t}{p_{t_{CL}}} \left(\frac{V}{V_{CL}}\right)^2$$

(15)

Normalized mass flux is obtained from the product of normalized density and velocity.

$$\frac{mf}{mf_{CL}} = \frac{\rho}{\rho_{CL}} \left(\frac{V}{V_{CL}}\right)$$

(16)

The normalized enthalpy is taken directly from the energy equation where gravitational effects are neglected and the static enthalpy is assumed to be much less than total enthalpy, which results in the following equation.

10

$$\frac{h}{h_{CL}} = \left(\frac{V}{V_{CL}}\right)^2 \tag{17}$$

Equations (14), (15), (16), and (17) were used in the code PROFILE to calculate the characteristic profiles of the arcjet high enthalpy flows using survey data.

11

V. RESULTS

For high-powered, arc-heated, hypersonic facilities the testing for aerodynamic or thermodynamic (heat transfer) studies requires a central core flow with properties well characterized. Ideally, of course, constant core flow properties are desirable. The present study was undertaken to characterize the flow properties of the 60-MW arc heated wind tunnel at NASA-Ames Research Center. Such flow properties are essential to the engineer for interpretation of the results for aero-thermodynamic tests.

Arc heaters operate with a large enthalpy gradients near the walls. These gradients cause the flow properties in the central core to vary; and are an important concern in simulation in these ground-based test facilities. The degree of this variation has not been reported up to the present time for the arcjet facility at NASA-Ames Research Center. Enthalpy gradients are inherent in all types of arc heaters that operate with cooled walls. For example, the temperature ratio of the wall for a typical arc heater varies from 2 - 5 % when the enthalpy level is in the typical vehicle reentry range of 18.6 - 41.87 MJ/kg (8000-18000 Btu/lb_m) which in terms of velocity equates to 20,000-30,000 ft/sec. The constricted arc heater was developed to minimize this gradient by the current density and length to cause the enthalpy profile to assume a flatter shape than a free-burning or vortex-stabilized arc heater. The theory of Stine-Watson [Ref. 3] shows that for a constricted arc heater the enthalpy profile assumes a Bessel function form as opposed to a linear profile for a free-burning or vortex-stabilized design (Huels arc) illustrated in Figure 11.

Results from the profile measurements obtained here can be used to answer the question as to whether the property variables (enthalpy, velocity, density and

12

energy flux) have the same profile or shape at the nozzle exit as they do for the constrictor. Scant measurements exist for the constrictor. Most of the values for the constrictor arc heaters are predicted by the Stine-Watson theory. Elaboration of this theory is represented by a computer code called ARCFLO II [Ref. 4]. This code was developed to predict the performance of high-pressure, high-enthalpy constricted-arc heaters. The conservation equations (mass, axial momentum, and energy) are written for a steady-state and radiatively participating gas mixture with electric current conduction. The governing equations employ the boundary-layer approximation and, hence, the pressure in the wall normal direction is assumed constant. Auxiliary relations, such as the equation of state, global current continuity, and global mass continuity, are used to relate the gas density with the pressure, mass flow rate, and mixture properties.

The profiles of density, velocity, enthalpy and energy flux computed by ARCFLO II in the constrictor are compared with experimental survey data obtained at the nozzle exit in Figure 12. The difference seen in the density profiles, Figure 12a, can be accounted for by the increase in density near the wall of the constrictor as opposed to the decrease in density in an expanding free jet. The velocity profiles, Figure 12b, are very similar with the experimental data showing a slightly flatter profile. The enthalpy profiles, Figure 12c, shows for ARCFLO II a central core region where the enthalpy drops moderately from the centerline to r/R = 0.4, a linearly decreasing region to r/R = 0.95, and then a steep drop near the wall where the conduction losses dominate. The ratio of centerline enthalpy to mass average enthalpy is 1.6. This low ratio value is typical for wall-stabilized arcs. The survey data exhibits a much flatter profile than ARCFLO II with a ratio of centerline enthalpy to mass average enthalpy of 1.15.

13

The product of the above three profiles is shown in Figure 12d and is the energy flux of the airstream. Note that this parameter is proportional to the convective heat-transfer rate to a body within the stream and that it is a measure of the usable stream area. The flat profile for ARCFLO II implies that stagnation point heating to a test body would be constant to within 10 % of the value obtained on the centerline flow for r/R up to 0.7. The survey data profile shows a more pronounced curve which can be attributed to the decrease in density in the free jet. If test chamber static pressure is maintained at the nozzle exit static pressure then the density profile would become flatter and thereby improve the energy flux profile.

Figures 13 - 28 are plots of PROFILE code output data at specified survey test points. All test point plots are normalized with respect to the corresponding values obtained at the 3-inch downstream positions.

14

VI. CONCLUSIONS AND RECOMMENDATIONS

The present study of survey data for the 13-inch IHF nozzle showed:

-   That there is good agreement between the ARCFLO II code prediction for velocity profile and experimental data;

-   Enthalpy profile of experimental data is much flatter than ARCFLO II theory predicts, which can be explained by the codes inability to account for energy transfer toward constrictor edges.

It is recommended that:

-   Future surveys control test chamber conditions in order to determine if improvements in the profile characteristics result;

-   Sting mounted heat transfer and stagnation pressure probes be developed in order to reduce probe mount interference with boundary layer of the flow;

-   Survey data be organized into accessible files so that characteristic maps for individual nozzles and complete nozzles can be utilized by researchers and contractors.

APPENDIX A

DERIVATION OF THE CLOSED FORM OF THE FAY-RIDDELL EQUATION

by WARREN WINOVICH

1. The Nusselt number is defined by:

$$Nu = \frac{H_x}{k_w} \quad (w = \text{wall value}) \tag{A1}$$

2. The heating rate is given by:

$$\dot{q} = H(T_s - T_w) = \frac{H(h_s - h_w)}{c_{p_w} c} \tag{A2}$$

where

$$c = \frac{\bar{c}_p}{c_{p_w}} \qquad \bar{c}_p = \frac{h_s - h_w}{T_s - T_w} = 1$$

(by definition of Nusselt number; wall temperature used as reference)

3. Solving for heating rate in terms of Nusselt number.

$$\dot{q} = \frac{Nu\, k_w}{x} \frac{(h_s - h_w)}{c_{p_w} c} \tag{A3a}$$

$$\dot{q} = \frac{Nu}{\sqrt{\dfrac{u_e \rho_w x}{\mu_w}}} \sqrt{\frac{u_e}{x}} \sqrt{\rho_w \mu_w} \frac{1}{\left(\dfrac{\mu_w c_{p_w}}{k_w}\right)} \frac{(h_s - h_w)}{c} \tag{A3b}$$

where subscript "e" indicates external flow conditions

16

$$q = \frac{Nu}{\sqrt{Re}} \sqrt{\frac{u_e}{x}} \sqrt{\rho_w \mu_w} \frac{(h_s - h_w)}{Pr_w\, c} \tag{A3c}$$

4. For the laminar boundary layer near the stagnation point:

$$u_e = \left(\frac{d\, u_e}{d\, x}\right)_s x \tag{A4a}$$

therefore

$$q = \frac{Nu}{\sqrt{Re}} \sqrt{\left(\frac{d\, u_e}{d\, x}\right)_s} \sqrt{\rho_w \mu_w} \frac{(h_s - h_w)}{Pr_w\, c} \tag{A4b}$$

5. Evaluation of velocity gradient at the stagnation point for a hemisphere:

$$p_e + \frac{1}{2} \frac{\rho_e}{g_c} u_e^2 = p_{t_2} \qquad (\text{momentum equation})$$

$$u_e = \sqrt{\frac{2 g_c\, p_{t_2}}{\rho_e}\left(1 - \frac{p_e}{p_{t_2}}\right)} \tag{A5a}$$

$$\frac{p_e}{p_{t_2}} = 1 - \sin^2\left(\frac{x}{R}\right) \qquad (\text{Newtonian flow over hemisphere})$$

$$u_e = \sqrt{\left(\frac{p_{t_2}}{\rho_e}\right)} \sin\left(\frac{x}{R}\right) \tag{A5b}$$

$$\left(\frac{d\, u_e}{d\, x}\right) = \frac{1}{R} \sqrt{2 g_c\left(\frac{p_{t_2}}{\rho_e}\right)} \cos\left(\frac{x}{R}\right) \tag{A5c}$$

17

$$\left(\frac{d\,u_e}{d\,x}\right)_e = \frac{1}{R}\sqrt{2\,g_c\!\left(\frac{P_{t_2}}{\rho_{t_e}}\right)}\,1 \qquad \rho_e = \rho_{t_e} \quad \text{for} \quad x = 0 \tag{A5d}$$

6. The heating rate equation becomes:

$$\dot{q} = \frac{Nu}{\sqrt{Re}}\,\sqrt{\rho_w \mu_w}\,\frac{1}{\sqrt{R}}\sqrt{2\,g_c\!\left(\frac{P_{t_2}}{\rho_{t_e}}\right)}\frac{(h_s - h_w)}{Pr_w\,c} \tag{A6}$$

7. The Fay and Riddell result for the heating transfer coefficient is:

$$\frac{Nu}{\sqrt{Re}} = 0.763(Pr)^{0.4}\left(\frac{\rho_s \mu_s}{\rho_w \mu_w}\right)^{0.4} c \tag{A7}$$

(equation 63 and 45 Fay and Riddell)

8. Substituting equation (A7) into equation(A6); using

$$\sqrt{\left(\frac{P_{t_2}}{\rho_{t_e}}\right)} = \sqrt[4]{R\,T_s Z_s} \qquad \text{and} \quad R = 53.5$$

gives:

$$\dot{q} = 0.763(Pr)^{-0.6}\sqrt[4]{2\,g_c(53.3)}\sqrt{\rho_w \mu_w}$$
$$\left(\frac{\rho_s \mu_s}{\rho_w \mu_w}\right)^{0.4}\sqrt[4]{T_s Z_s}\,\frac{(h_s - h_w)}{\sqrt{R}} \tag{A8a}$$

$$\frac{\dot{q}\sqrt{R}}{(h_s - h_w)} = \frac{0.763}{(Pr)^{-0.6}}\sqrt[4]{2\,g_c(53.3)}\sqrt{\rho_s \mu_s}\left(\frac{\rho_w \mu_w}{\rho_s \mu_s}\right)^{0.1}\sqrt[4]{T_s Z_s} \tag{A8b}$$

18

9. Using:

$$\rho_s = 39.65 \frac{p_s}{T_s Z_s} \tag{A9a}$$

$$\mu_s = 184 \times 10^{-7} \left(\frac{T_s}{1000}\right)^{0.628} K_s \tag{A9b}$$

where

$$K = \frac{\mu_{exact}}{\mu_{formula}}$$

Equation (A9b) is appropriate for temperatures of 6000°K (10000°R) where arcjet operate and for reentry and reentry stagnation conditions ($V_{entry} > 5000$ m/sec ~ 15000 ft/sec)

$$\rho_s \mu_s = \frac{39.65 \times 184 \times 10^{-7}}{1000^{0.628}} \frac{p_s T_s^{0.628}}{T_s Z_s} K_s$$

$$\frac{\rho_s \mu_s}{p_s} = 9.60 \times 10^{-6} \frac{T_s^{0.628}}{T_s Z_s} K_s \tag{A9c}$$

$$\frac{\rho_w \mu_w}{\rho_s \mu_s} = \frac{T_s Z_s}{T_w Z_w} \frac{T_w^{0.628}}{T_s^{0.628}} \frac{K_w}{K_s} \tag{A9d}$$

Note that $K_w = 1.00$ for the expression chosen for viscosity.

10. The final form for the expression for heating rate becomes:

$$\frac{\dot{q}\sqrt{R}}{\sqrt{p_s}(h_s - h_w)} = \frac{0.763}{(Pr)^{-0.6}} \sqrt[4]{2g_c(53.3)}\, 3.10 \times 10^{-3} \frac{(T_s Z_s)^{0.25} T_s^{0.314}}{(T_s Z_s)^{0.5}}$$
$$K_s \left(\frac{T_s Z_s}{T_w Z_w}\right)^{0.1} \left(\frac{T_w}{T_s}\right)^{0.0628} \left(\frac{K_w}{K_s}\right)^{0.1} \tag{A10a}$$

Simplifying for Pr = 0.71 the equation becomes:

$$\frac{\dot{q}\sqrt{R}}{\sqrt{p_s}(h_s - h_w)} = \{\text{constant}\}\,\frac{(T_s Z_s)^{-0.15}T_s^{0.251}K_s^{0.4}}{(T_w Z_w)^{0.0372}}$$

$$\frac{\dot{q}\sqrt{R}}{\sqrt{p_s}(h_s - h_w)} = \{\text{constant}\}\,\frac{(T_s Z_s)^{0.101}}{(T_w Z_w)^{0.0372}}\left(\frac{Z_w}{Z_s}\right)^{0.251}K_s^{0.4}$$

Noting that $Z_w = 1.00$

For Pr = 0.71 the constant in brackets above becomes:

$$\{\text{constant}\} = \frac{0.763}{(Pr)^{-0.6}}\,\sqrt[4]{2g_c(53.3)}\;3.10\times 10^{-3}\qquad = 0.02225$$

and the expression for heating rate is:

$$\frac{\dot{q}\sqrt{R}}{\sqrt{p_s}(h_s - h_w)} = \{0.02225\}\left\{K_s^{0.4}\left(\frac{T_s Z}{T_w Z_w}\right)^{0.0372}\frac{(T_s Z_s)^{0.0638}}{\left(\dfrac{Z_s}{Z_w}\right)^{0.251}}\right\}\tag{A10b}$$

The term within the braces is only a function of the stagnation state. For usual wind tunnel tests the stagnation state is within the limits:

$$0.01 < p_s < 1 \text{ atmosphere} \qquad 130 < h_s < 20,000 \text{ Btu/lb}_m$$

For this range of pressure and enthalpy the term in the braces is essentially a constant:

$$\left\{K_s^{0.4}\left(\frac{T_s Z}{T_w Z_w}\right)^{0.0372}\frac{(T_s Z_s)^{0.0638}}{\left(\dfrac{Z_s}{Z_w}\right)^{0.251}}\right\} = 1.873 \pm 0.042$$

Therefore the hemisphere formula for heating rate is:

$$\frac{\dot{q}\sqrt{R}}{\sqrt{p_s}\,(h_s - h_w)} = \{0.02225\}\{1.873\} = 0.0417$$

or:

$$\dot{q} = 0.0417\sqrt{\frac{p_s}{R}}\,(h_s - h_w) \qquad\qquad\text{(A10c)}$$

where

$\dot{q} = \text{Btu}/\text{s}\cdot\text{ft}^2$

$p_s = \text{atm} \quad \rightarrow \quad p_{t_2}\ (\text{measured})$

$R = \text{feet}$

$h = \text{Btu}/\text{lb}_m$

Symbols		Subscripts	
c_p	Specific heat	e	External Conditions
h	Entahlpy	s	Stream Conditions
k	Thermal Conductivity	t	Stagnation Conditions
Pr	Prandtl Number	w	Wall Conditions
R	Radius		
T	Temperature		
Z	Compressibilty Factor		
ρ	Density		
μ	Viscosity		

21

APPENDIX B

UNCERTAINTY ANALYSIS FOR DERIVATIONS

Uncertainty analysis of the heat transfer and stagnation pressure probes is based on manufacture's claims for uncertainties. In the case of the heat transfer probe the manufacturer list's accuracy of readings between 3 & 4 % of the value recorded. For the following analysis the value of 5 % is used. The accuracy of the stagnation pressure probe has been found by NASA personnel to be on the order of 1/4 % of the recorded value. Using these values the uncertainty of the normalized velocity is shown below.

Starting with equation (14):

$$\left(\frac{V}{V_{CL}}\right)^4 = \left(\frac{\dot{q}}{\dot{q}_{CL}}\right)^2 \left(\frac{p_t}{p_{t_{CL}}}\right)^{-1}$$

and taking the logarithmic differential gives:

$$\ln \frac{V}{V_{CL}} = \frac{1}{2} \ln\left(\frac{\dot{q}}{\dot{q}_{CL}}\right) - \frac{1}{4} \ln\left(\frac{p}{p_{CL}}\right)$$

Integrating

$$\frac{dV}{V_{CL}} = \frac{1}{2}\left(\frac{d\dot{q}}{\dot{q}} - \frac{d\dot{q}_{CL}}{\dot{q}_{CL}}\right) - \frac{1}{4}\left(\frac{dp}{p} - \frac{dp_{CL}}{p_{CL}}\right)$$

$$\frac{dV}{V_{CL}} = \frac{1}{2}\left[(e_r)\dot{q} - (e_r)\dot{q}_{CL}\right] - \frac{1}{4}\left[(e_r)p - (e_r)p_{CL}\right]$$

where (e_r) is uncertainty.

In the worst case where centerline values are opposite in sign of the original values results in

$$\frac{dV}{V_{CL}} = \frac{1}{2}[(0.05) - (-0.05)] - \frac{1}{4}[(0.0025) - (-0.0025)]$$

$$\frac{dV}{V_{CL}} = \frac{1}{2}[0.10] - \frac{1}{4}[0.005]$$

so that

$$\frac{dV}{V_{CL}} \pm 5\%$$

Applying the velocity uncertainty to the other property equations (15), (16) and (17) gives:

$$\frac{dh}{h_{CL}} = 2\left(\frac{dV}{V_{CL}}\right) \pm 10\%$$

$$\frac{d\rho}{\rho_{CL}} = \left(\frac{dp}{p}\right)\left[2\left(\frac{dV}{V_{CL}}\right)\right]^{-1} \pm 10\%$$

$$\frac{d\,mf}{mf_{CL}} = \left(\frac{d\rho}{\rho}\right)\left(\frac{dV}{V_{CL}}\right) \pm 15\%$$

23

APPENDIX C

COMPUTER PROGRAM FOR DETERMINING PROFILES

FILE: PROF2   FORTRAN A1

```
       PROGRAM PROFILE
C      THIS PROGRAM IS DESIGNED TO CALCULATE FLOW PROFILES FOR
C      NASA AMES IHF ARCJET WIND TUNNELS.  VELOCITY, DENSITY, MASS FLUX
C      AND ENTHALPY PROFILES NORMALIZED TO CENTERLINE CONDITIONS
C      ARE DEVELOPED.

       DIMENSION QDOT(1000), QDOTN(1000), PTOT(1000), VNOR(1000),
      &          RHO(1000), MFLUX(1000), HTOT(1000), DIST(1000),
      &          QSQR(1000), PTOTN(1000)
       REAL VNOR,RHO,MFLUX,HTOT,QSQR,PTOTN,QDOTN
       INTEGER S,I,J,K,L,IMAX,IQDOT,IPTOT,VAL,I1,I2
       REAL PMAX, QMAX,VMIN
       CHARACTER *36 G
       CHARACTER *1 E,Y,N
       CHARACTER *6 A,B,C
       CHARACTER *45 F
C      ****************************************************************
C      THIS SECTION COPIES TEST CONDITIONS INTO OUTPUT FILE
C      ****************************************************************
       READ(5,1)F
1      FORMAT(A45)
       WRITE(7,1)F
       READ(5,2)G,C
2      FORMAT(A36,A6)
       WRITE(7,*)G,C
       DO 10 I=1,3
          READ(5,1)F
          WRITE(*,1)F
          WRITE(7,1)F
10     CONTINUE
C      ****************************************************************
C      THIS NEXT SECTION READS TEST DATA FOR QDOT AND PTOT.
C      FIRST: NORMALIZES VALUES OF QDOT AND PTOT
C      SECOND: LOCATES MAXIMUM VALUE TO USE AS CENTERLINE
C      THIRD: CALCULATES VALUES FOR VELOCITY, DENSITY, MASS FLUX AND
C             ENTHALPY PROFILES NORMALIZED TO CENTERLINE
C
C      NOTE: QDOT AND PTOT DATA SHOULD CONTAIN ONLY ONE ZERO AS LAST
C            VALUE.  THIS IS CRITERIA USED TO TERMINATE READING OF DATA.
C
C      ****************************************************************
       IMAX=0
       DO 20 I=1,1000
          READ(5,15)QDOT(I), PTOT(I), DIST(I)
          IF(QDOT(I).EQ.0)GOTO 21
       IMAX=IMAX+1
20     CONTINUE
21     WRITE(*,*)'NUMBER OF DATA POINTS READ =',IMAX
       ENDFILE(5)
```

24

```
C       *******************************************************
C       1 NORMALIZATION OF QDOT AND PTOT
C       *******************************************************
        QMAX = 0
        PMAX = 0
        DO 200 I = 1,IMAX
            QMAX = MAX(QMAX,QDOT(I))
            PMAX = MAX(PMAX,PTOT(I))
  200   CONTINUE
C       *******************************************************
C       2 DETERMINING LOCATION OF MAX VALUES.  THESE WILL BE USED TO
C         ALIGN PROBE VALUES TO CENTERLINE.
C       *******************************************************

        DO 201 I=1,IMAX
            IQDOT=I
            VAL=DIM(QMAX,QDOT(I))
            IF(VAL.EQ.0)GOTO 202
  201   CONTINUE

  202   DO 203 I=1,IMAX
            IPTOT=I
            VAL1=DIM(PMAX,PTOT(I))
            IF(VAL1.EQ.0)GOTO 205
  203   CONTINUE
  205   WRITE(*,*)'I AT QMAX =',IQDOT,'  I AT PMAX =',IPTOT
C       *******************************************************
C       3 CALCULATION OF PROFILES
C       *******************************************************
        I1=IQDOT+179
        I2=IPTOT+179
        WRITE(*,*)'I1 =',I1,'   I2 =',I2
        K=0
        DO 300 I=IQDOT,I1
            K=K+1
            QDOTN(K)=ABS(QDOT(I)/QMAX)
            QSQR(K)=QDOTN(K)**2
  300       DIST(K)=DIST(I)-DIST(IQDOT)
        K=0
        DO 301 I=IPTOT,I2
            K=K+1
  301       PTOTN(K)=ABS(PTOT(I)/PMAX)
        DO 302 I=1,K
            VNOR(I) = SQRT(SQRT(QSQR(I)/PTOTN(I)))
            RHO(I) = PTOTN(I)/(1/VNOR(I))**2
            MFLUX(I) = RHO(I)*VNOR(I)
  302       HTOT(I) = VNOR(I)**2
        GOTO 400


  400   WRITE(7,*)'QMAX = ',QMAX
        WRITE(6,*)'QMAX = ',QMAX
        WRITE(7,*)'PMAX =',PMAX
        WRITE(6,*)'PMAX =',PMAX
        WRITE(7,*)'==================================================
       &==============='
        WRITE(7,*)'  HEATING    STAG    VELOCITY  DENSITY   MFLUX
       &ENTHPY     DIST'
        WRITE(7,*)'    RATE     PRESSURE'
        WRITE(7,*)'==================================================
       &==============='
        WRITE(7,600)(QDOTN(I),PTOTN(I),VNOR(I),RHO(I),MFLUX(I),HTOT(I),DIS
       &T(I),I=1,K,4)
  600   FORMAT(6(5X(F5.3)),5X,F6.3)
        STOP
        END
```

Figure 1 Schematic diagram of the 60 MW IHF.

Figure 2   Photograph of the 60 MW IHF with Mach 7.5 conical nozzle.

27
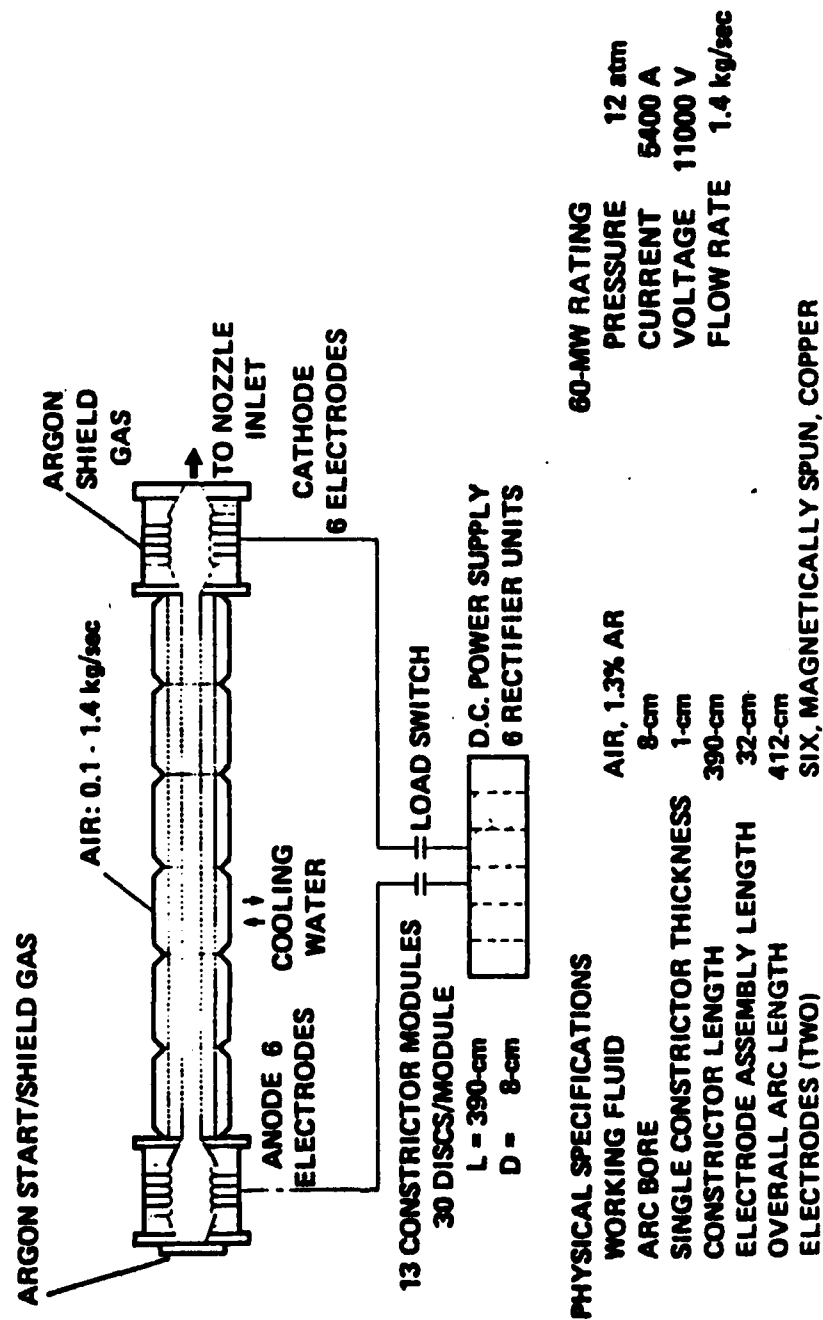
Figure 3   8-cm Constricted arc heater.
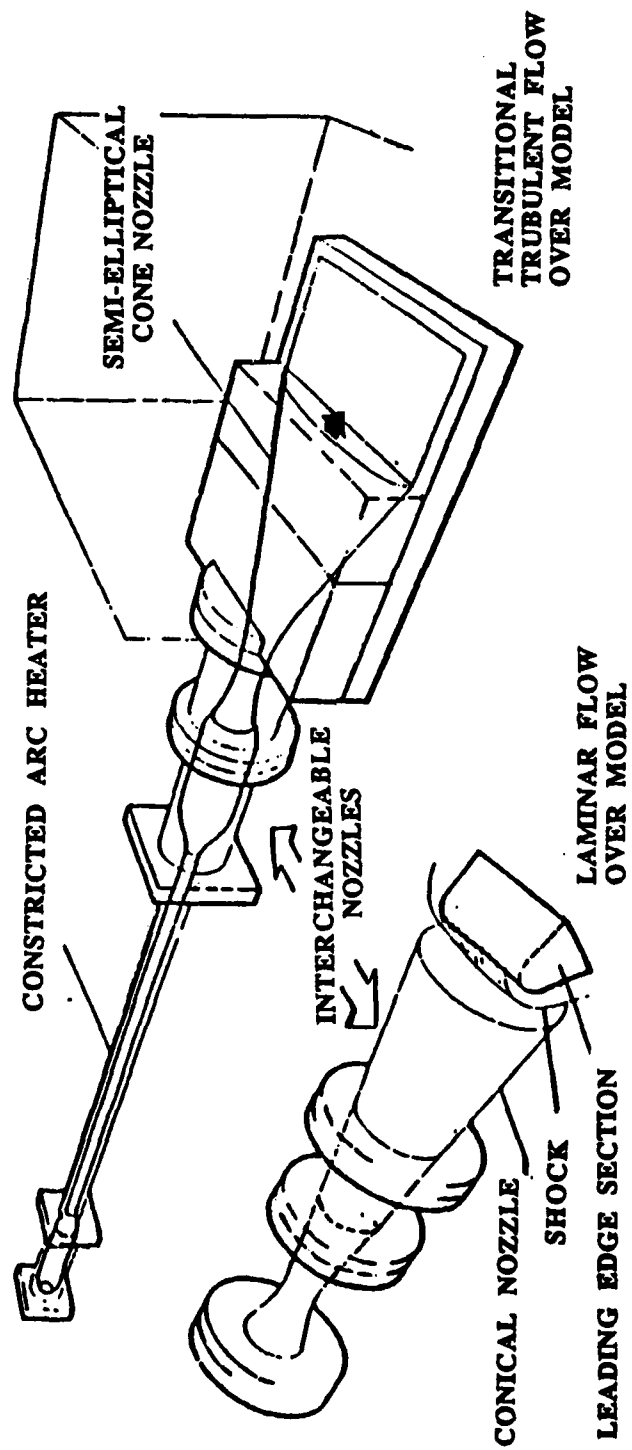
Figure 4 Diagram of interchangeable nozzles for the 60 MW IHF.

CONSTRICTED ARC HEATER

SEMI-ELLIPTICAL CONE NOZZLE

TRANSITIONAL TRUBULENT FLOW OVER MODEL

INTERCHANGEABLE NOZZLES

CONICAL NOZZLE

SHOCK

LEADING EDGE SECTION

LAMINAR FLOW OVER MODEL

Figure 5 Gardon type calorimeter probe.

Figure 6 Stagnation pressure probe - with support mount.
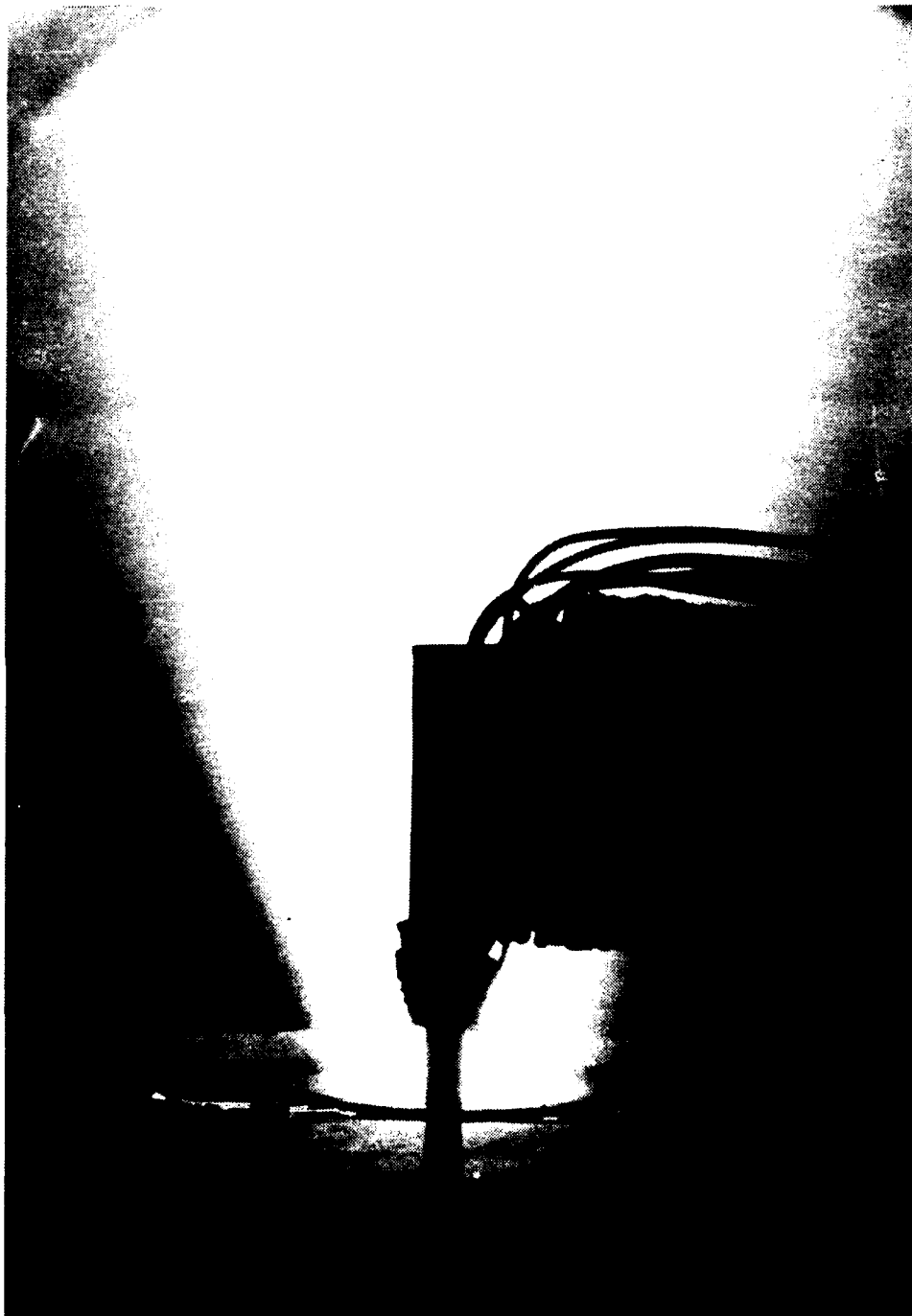
Figure 7 Probes and support mounts outside 6-inch nozzle free jet flow.

Figure 8   Probes entering 6-inch nozzle free jet flow during survey.

Figure 9 Probes near centerline of 6-inch nozzle free jet flow.
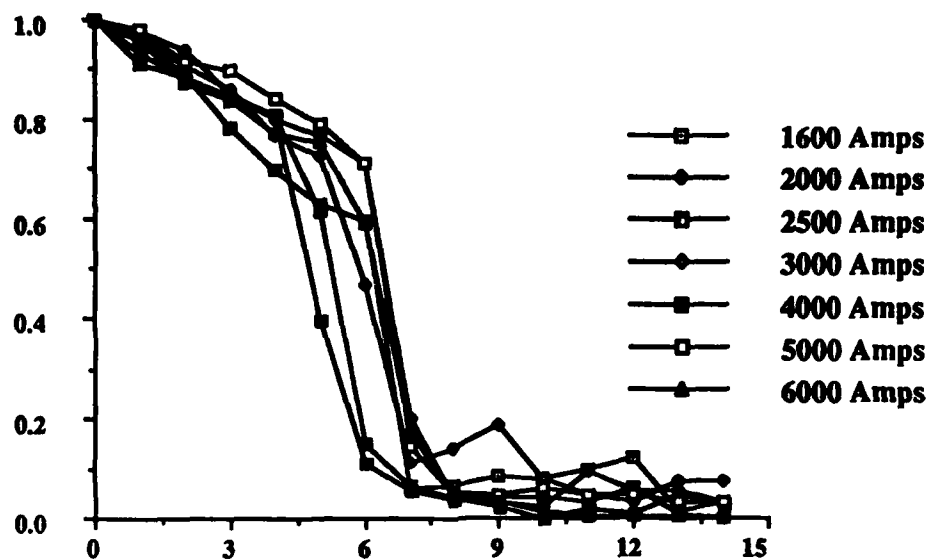
(a) Heat transfer rate verses radius at 3-inch
position from nozzle exit
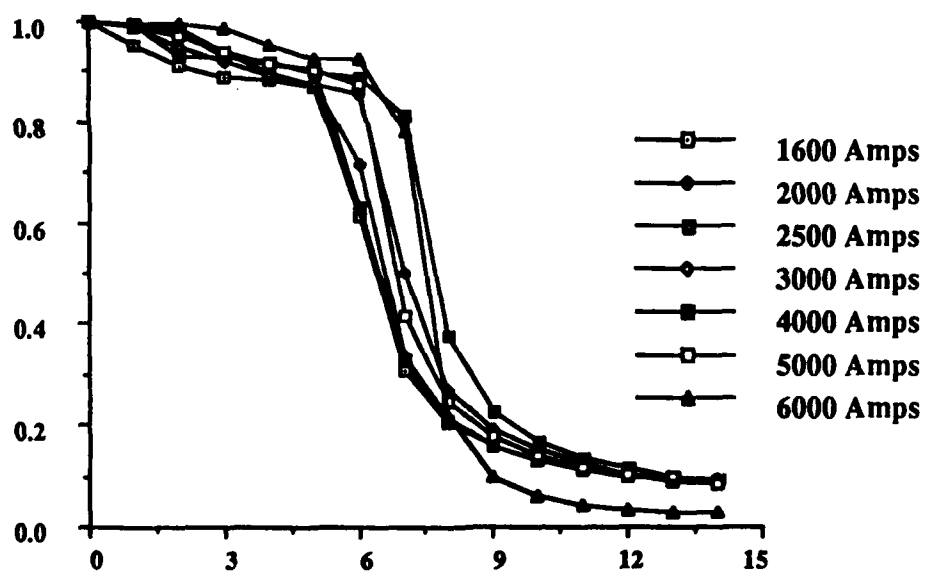
(b) Stagnation Pressure verses radius at 3-inch
position from nozzle exit

Figure 10   Typical profiles of the heat transfer rate
and stagnation pressure, 13-inch nozzle (A/A* = 30)

35
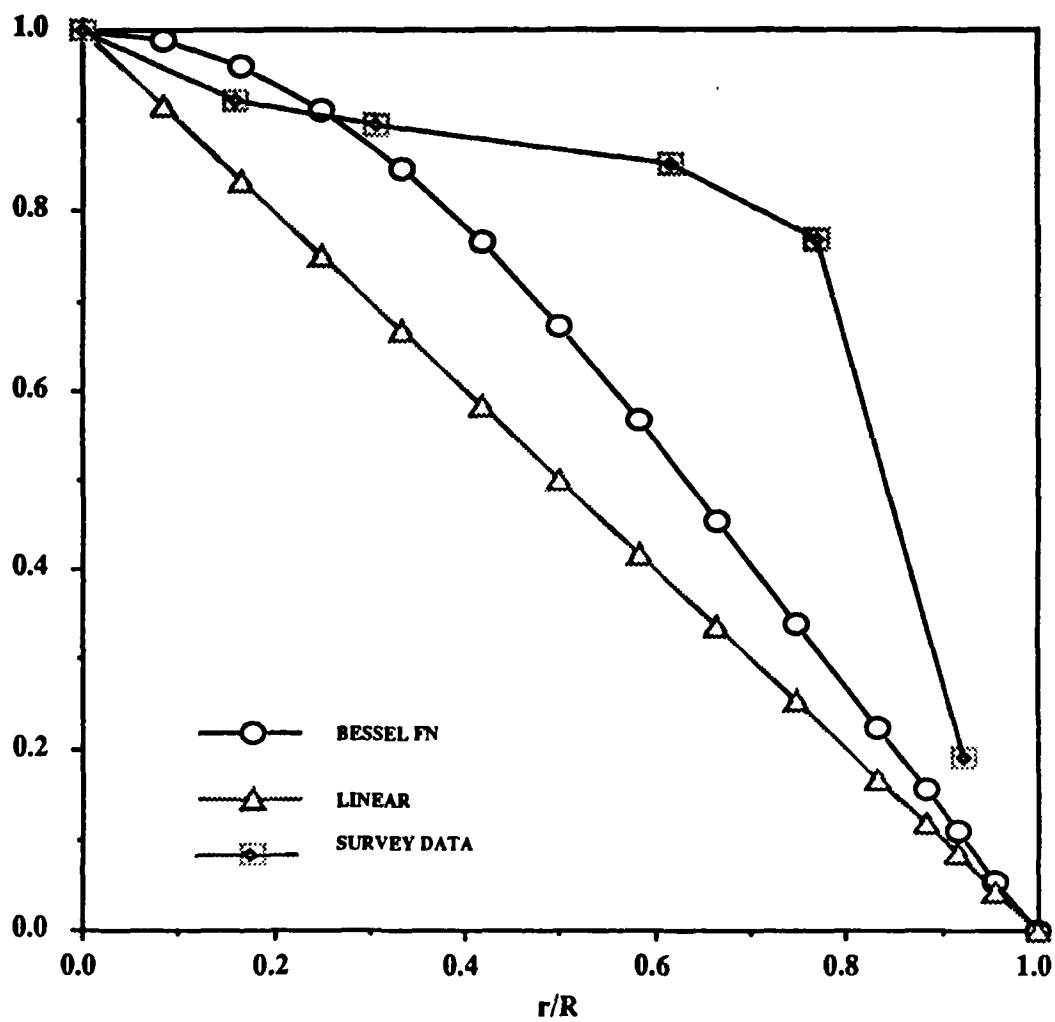
Figure 11 Comparison of enthalpy profiles for 8-cm constricted arc.

36
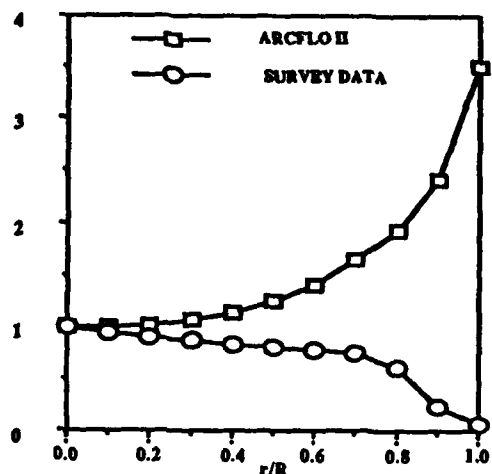
(a) Density Profile
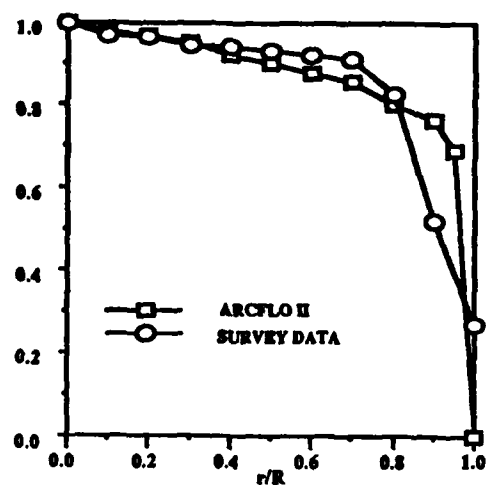
(b) Velocity Profile
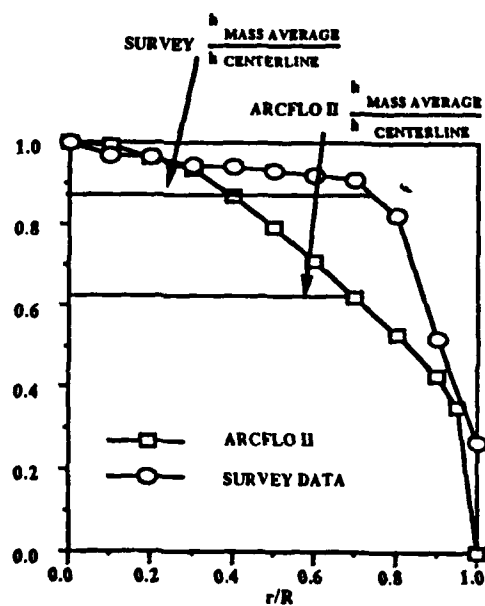
(c) Enthalpy Profile
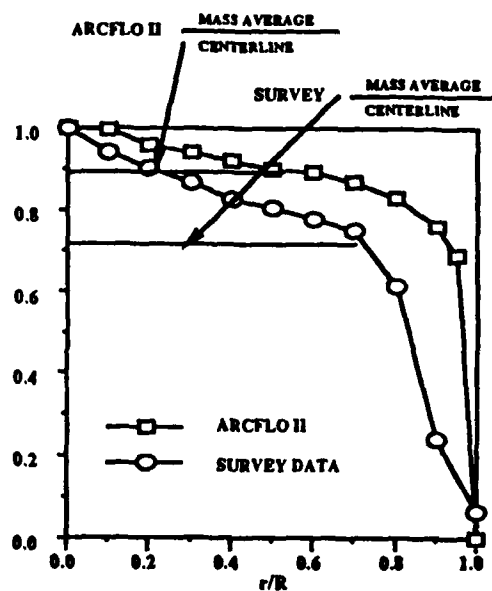
(d) Energy Flux Profile

Figure 12   Comparison of ARCFLO II and survey data profiles of 8-cm constricted arc.

37
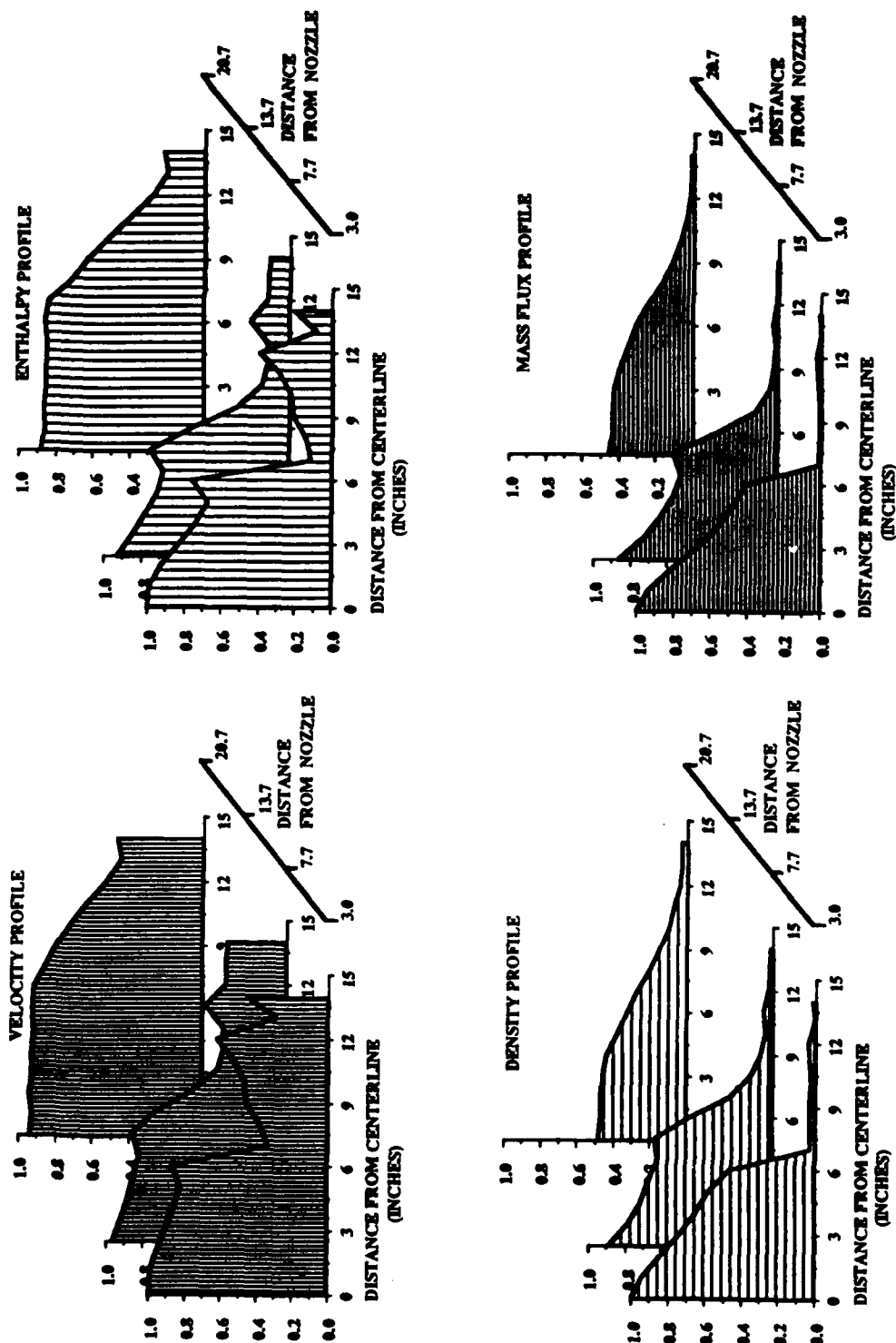
Figure 13   13-inch nozzle profiles normalized by 3-inch position from exit.
Constrictor conditions: 1600 Amps, 25 psia constrictor pressure, 6.0 MW arc power input.

38
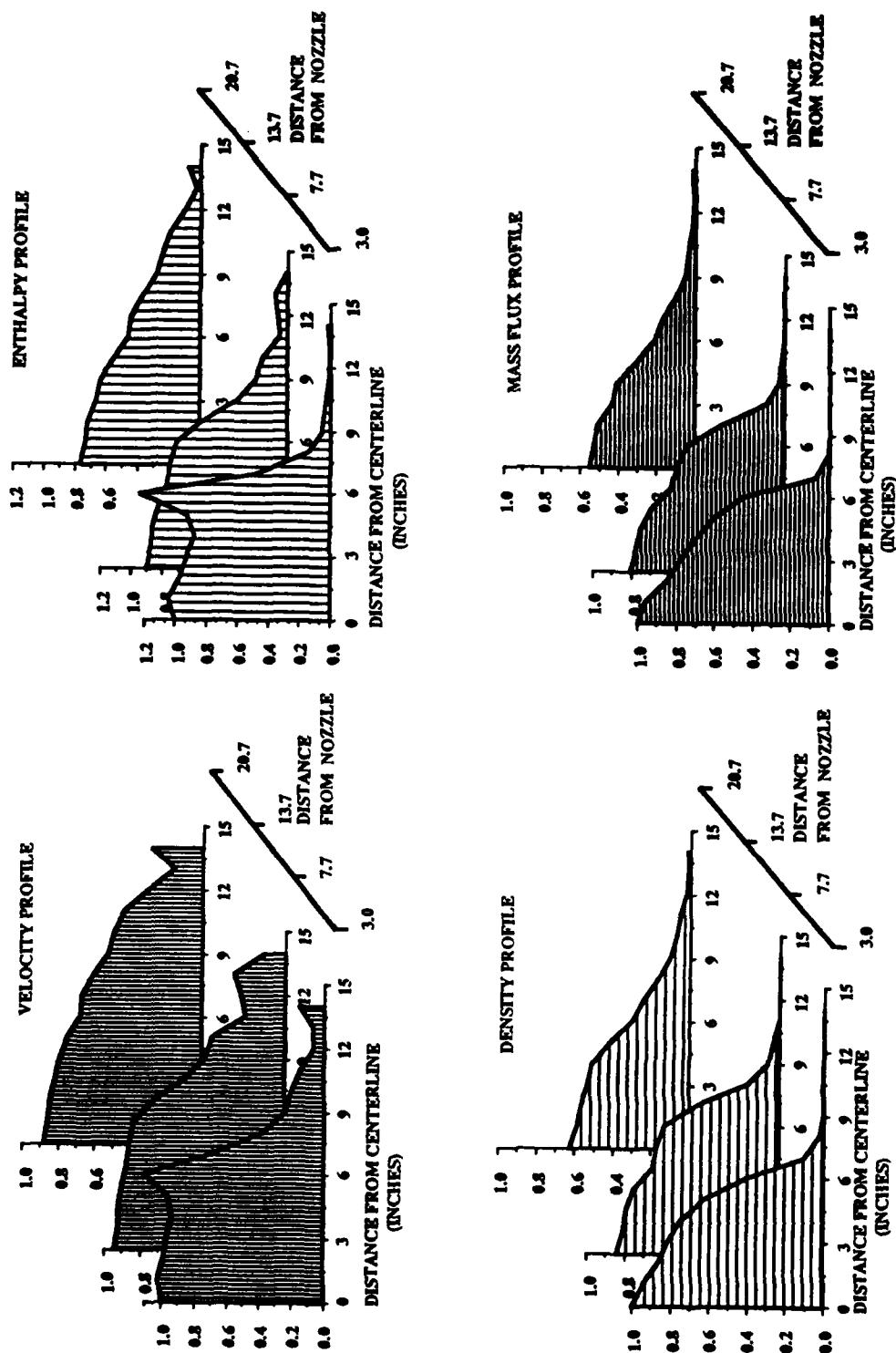
Figure 14   13-inch nozzle profiles normalized by 3-inch position from exit. Constrictor conditions: 2000 Amps, 27 psia constrictor pressure, 7.4 MW arc power input.
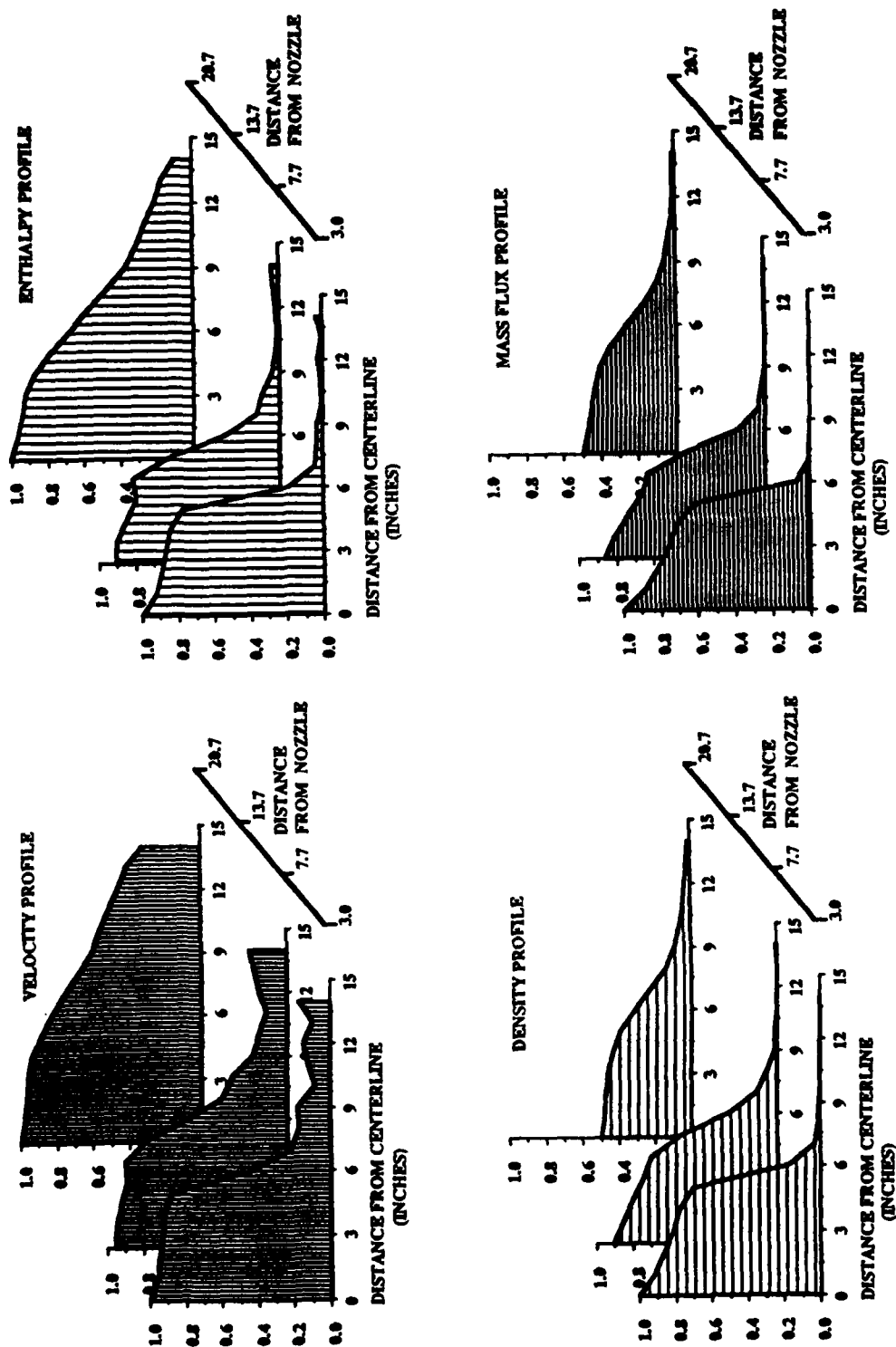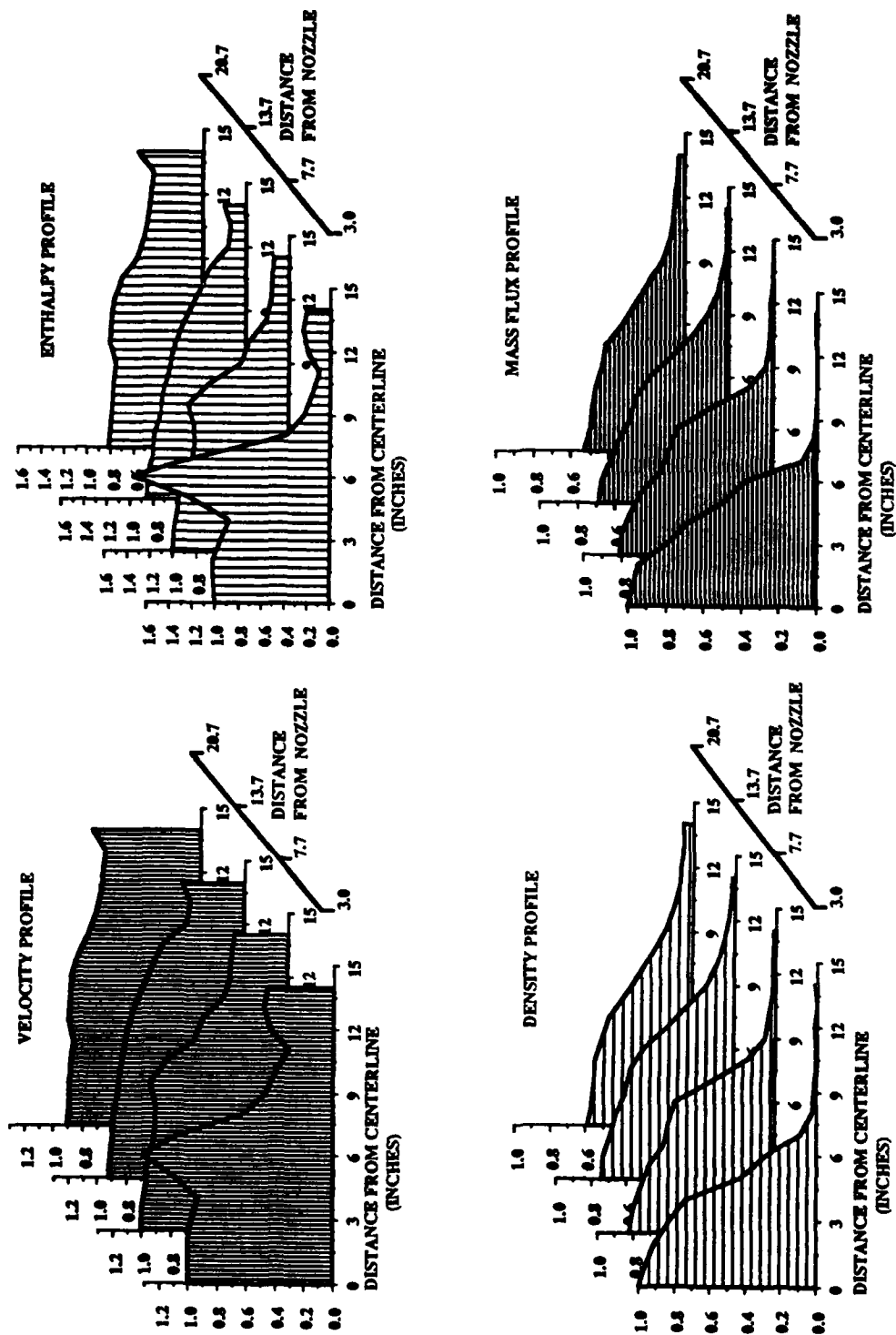
39
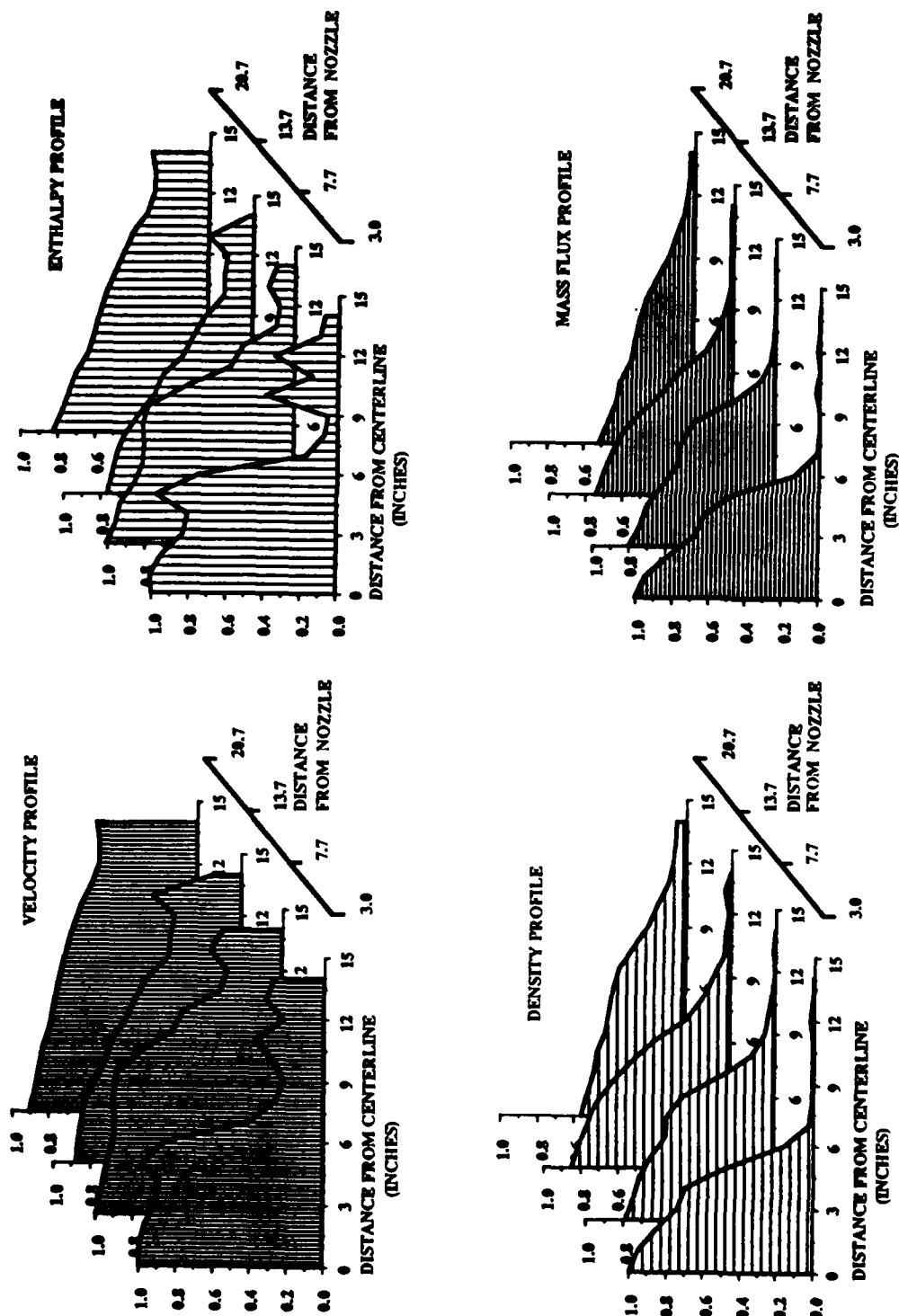
Figure 15 13-inch nozzle profiles normalized by 3-inch position from exit. Constrictor conditions: 2000 Amps, 46 psia constrictor pressure, 7.4 MW arc power input.
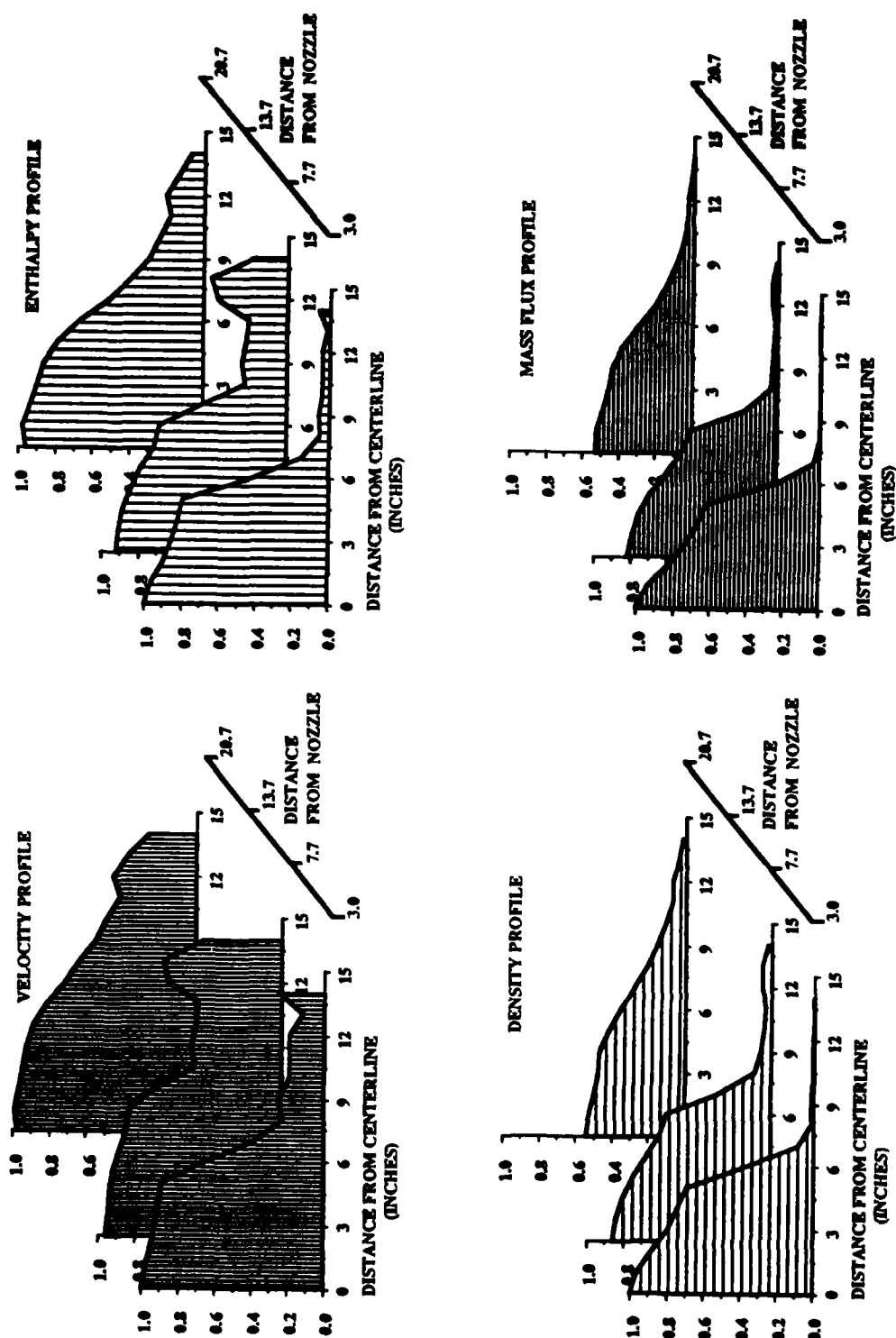
Figure 16 13-inch nozzle profiles normalized by 3-inch position from exit.
Constrictor conditions: 2500 Amps, 28 psia constrictor pressure, 9.3 MW arc power input.

41
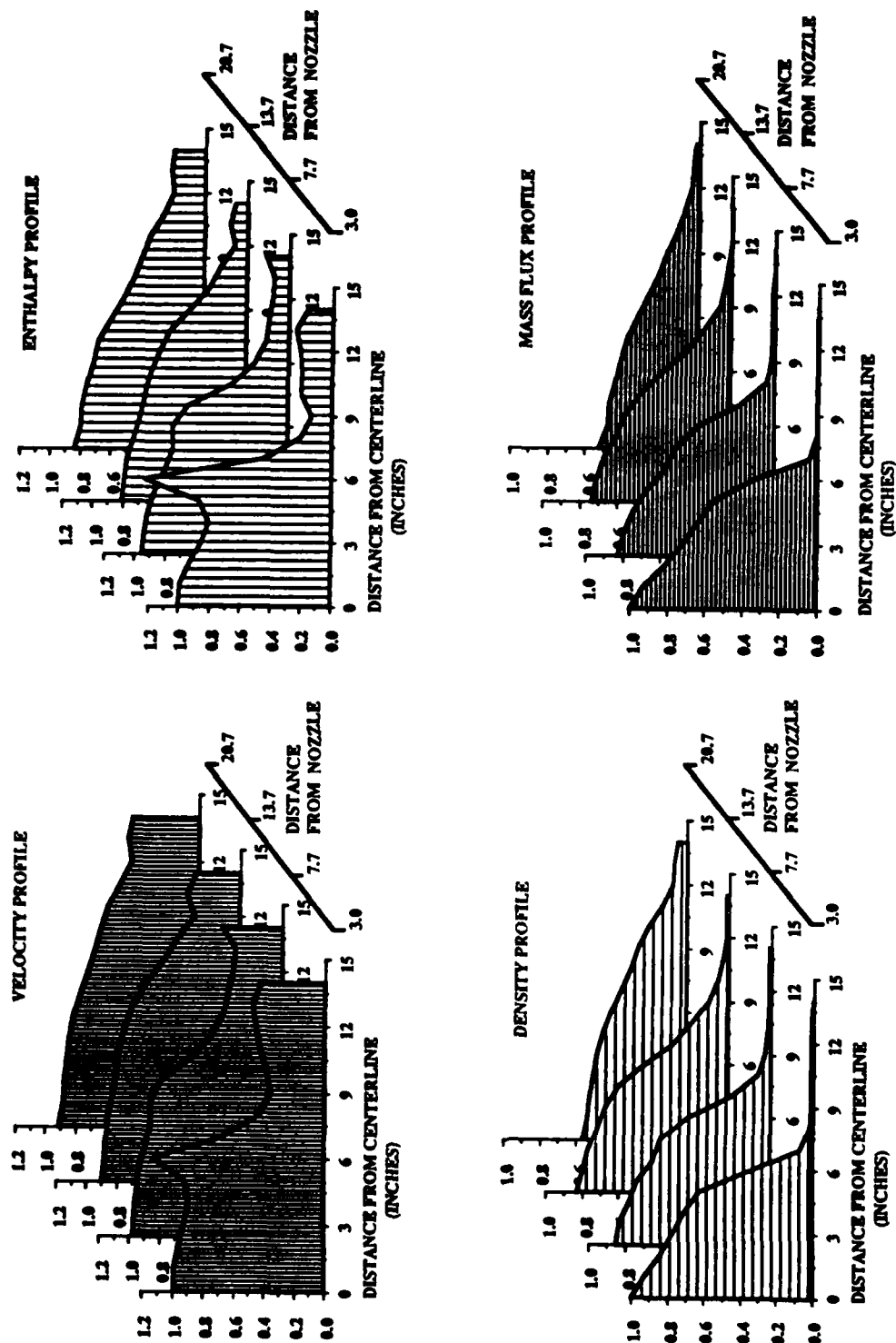
Figure 17 13-inch nozzle profiles normalized by 3-inch position from exit.
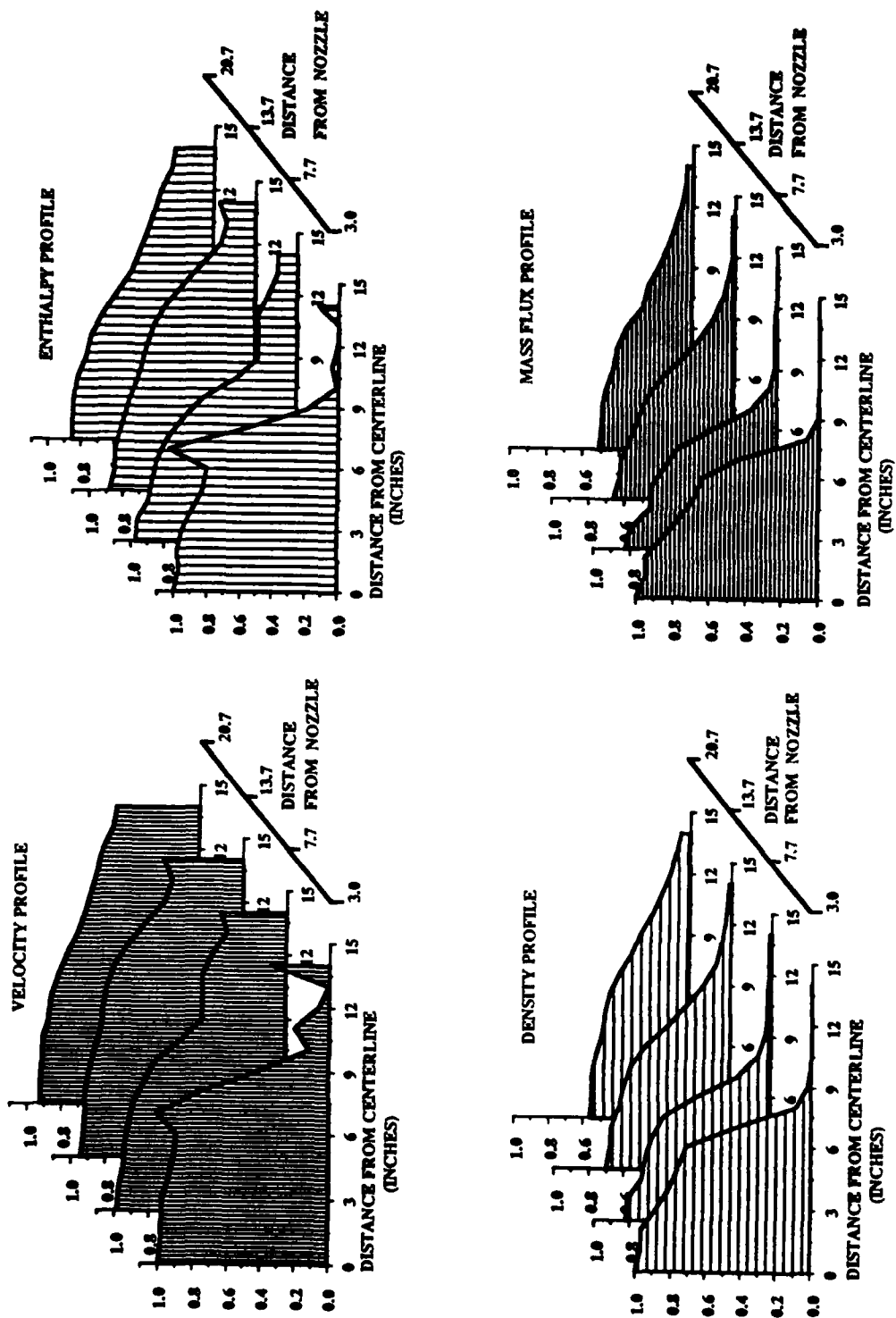Constrictor conditions: 2500 Amps, 48 psia constrictor pressure, 9.3 MW arc power input.
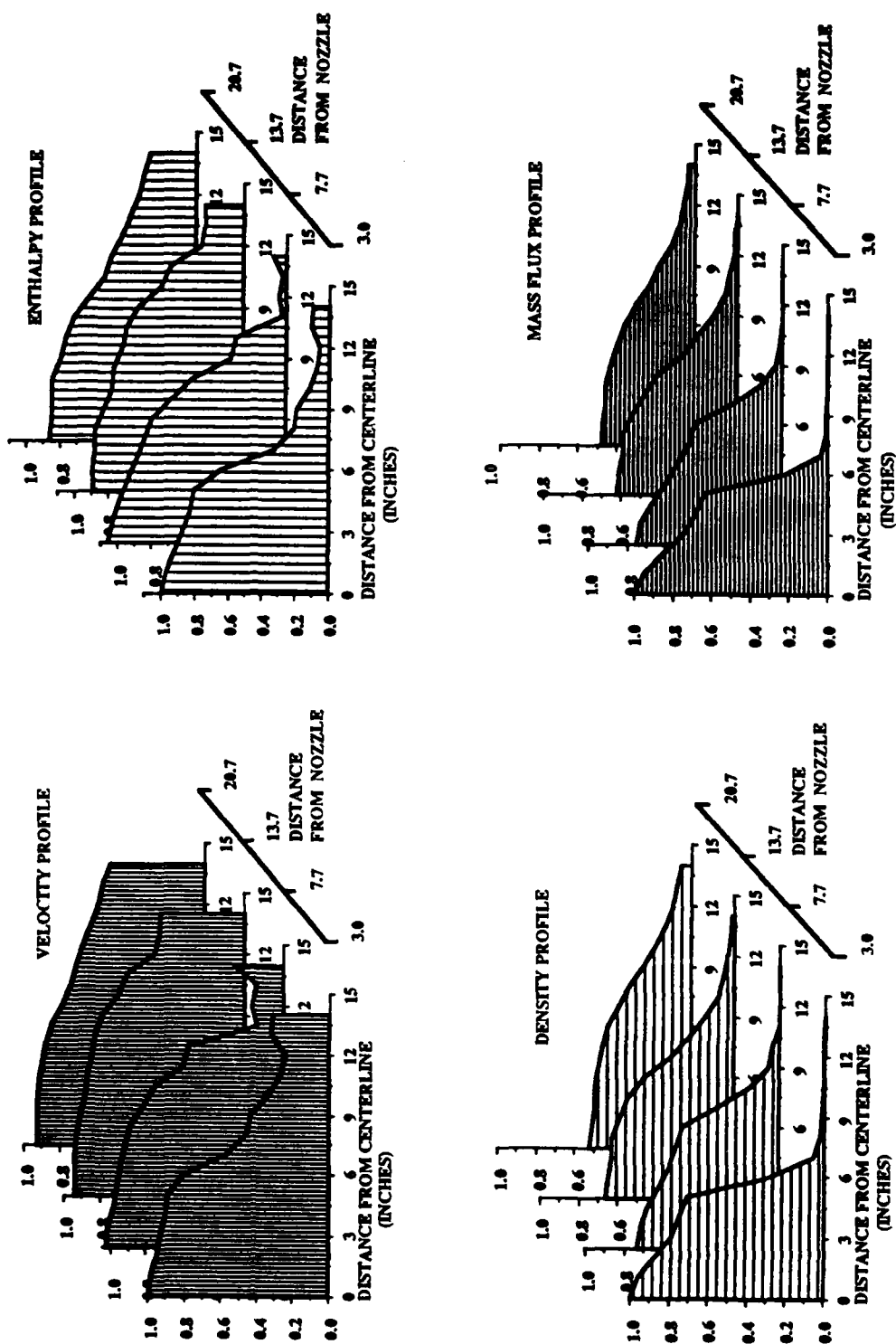
Figure 18   13-inch nozzle profiles normalized by 3-inch position from exit.
Constrictor conditions: 2500 Amps, 72 psia constrictor pressure, 9.3 MW arc power input.

Figure 19 13-inch nozzle profiles normalized by 3-inch position from exit. Constrictor conditions: 3000 Amps, 28 psia constrictor pressure, 11 MW arc power input.
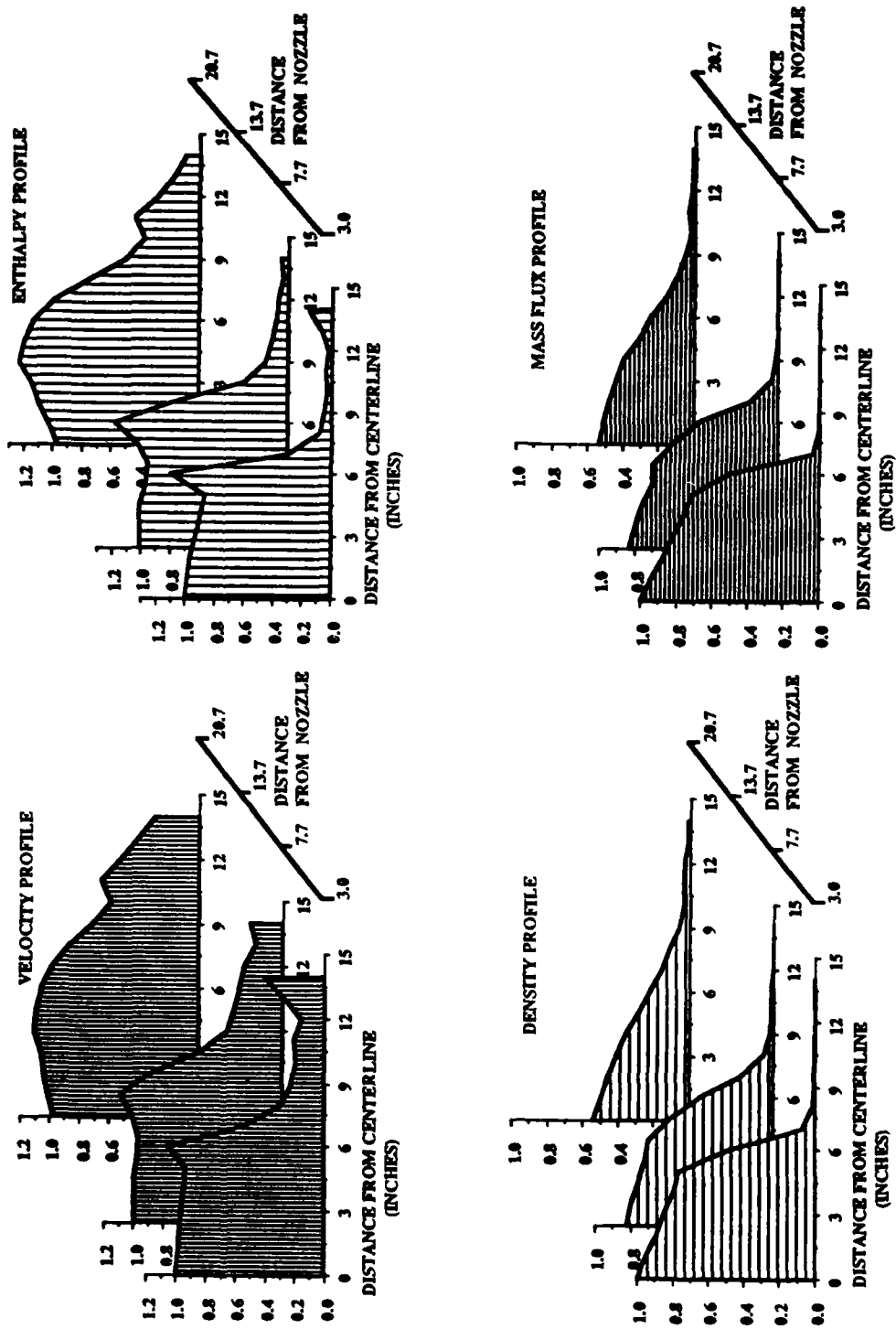
44

Figure 20 13-inch nozzle profiles normalized by 3-inch position from exit. Constrictor conditions: 3000 Amps, 49 psia constrictor pressure, 11 MW arc power input.

45

Figure 21   13-inch nozzle profiles normalized by 3-inch position from exit.
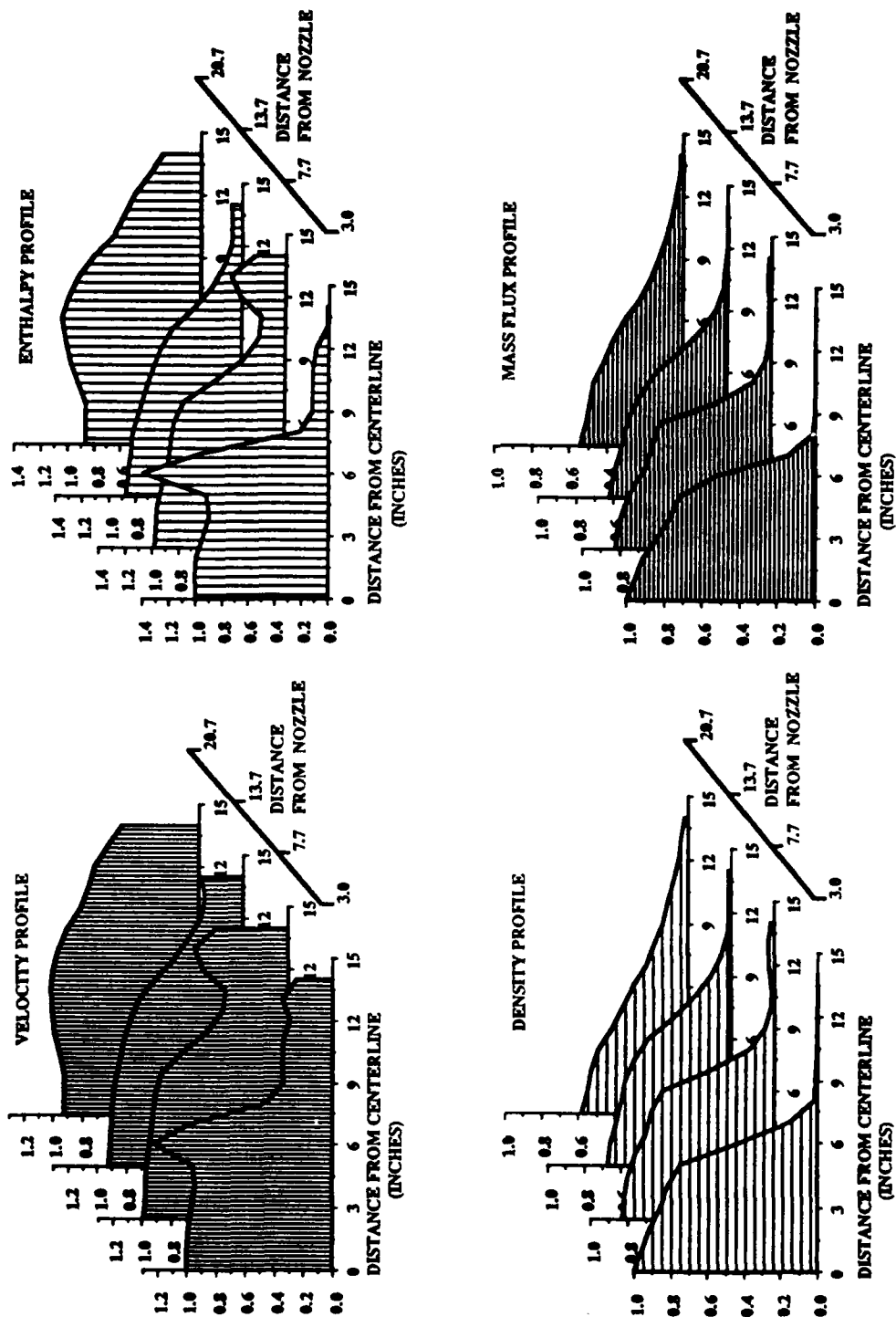Constrictor conditions: 3000 Amps, 73 psia constrictor pressure, 11 MW arc power input.

46

Figure 22   13-inch nozzle profiles normalized by 3-inch position from exit. Constrictor conditions: 4000 Amps, 30 psia constrictor pressure, 14.8 MW arc power input.

47

Figure 23   13-inch nozzle profiles normalized by 3-inch position from exit.
Constrictor conditions: 4000 Amps, 51 psia constrictor pressure, 14.8 MW arc power input.
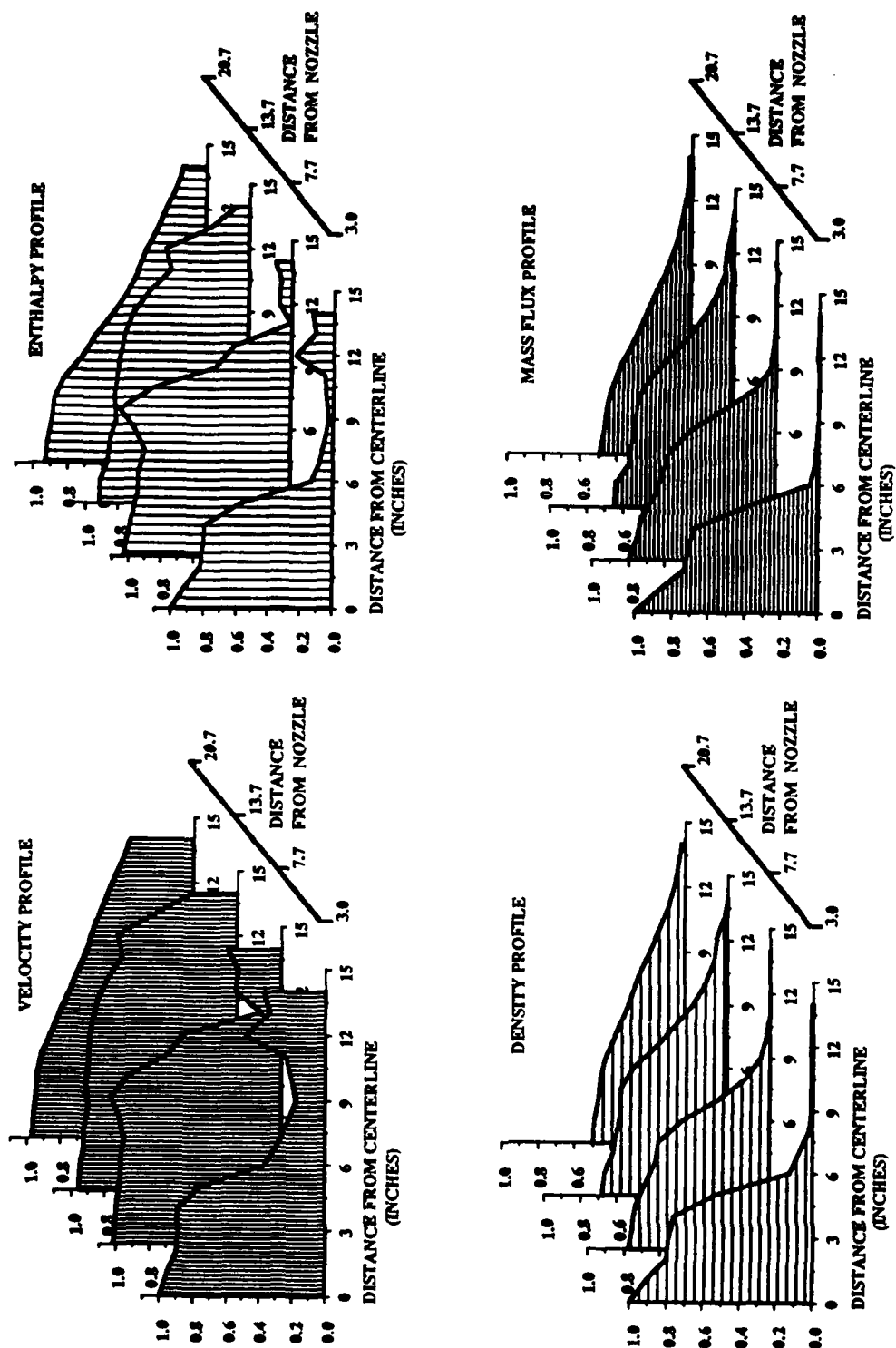
Figure 24 13-inch nozzle profiles normalized by 3-inch position from exit. Constrictor conditions: 4000 Amps, 75 psia constrictor pressure, 14.8 MW arc power input.
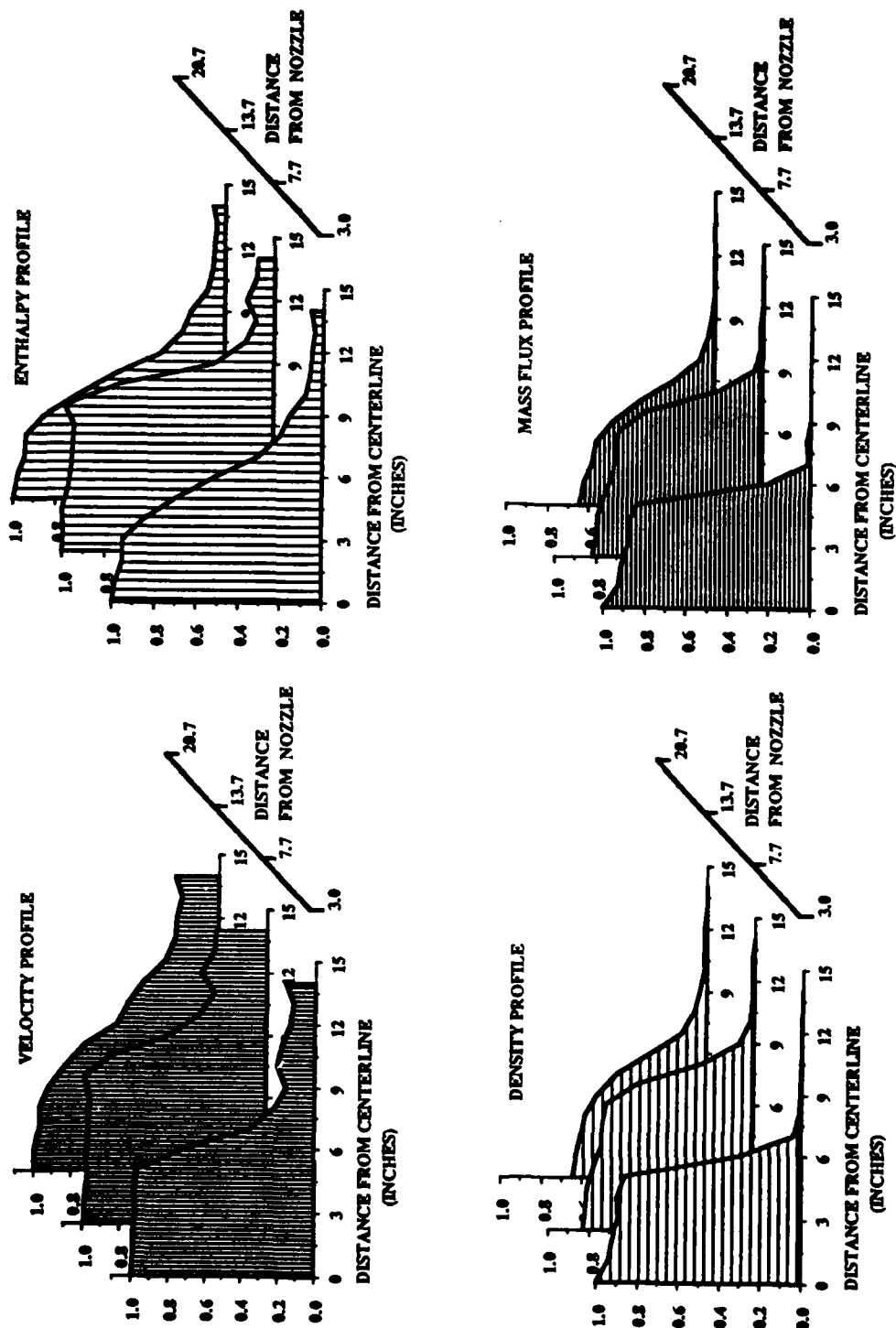
Figure 25 13-inch nozzle profiles normalized by 3-inch position from exit. Constrictor conditions: 5000 Amps, 31 psia constrictor pressure, 18.5 MW arc power input.
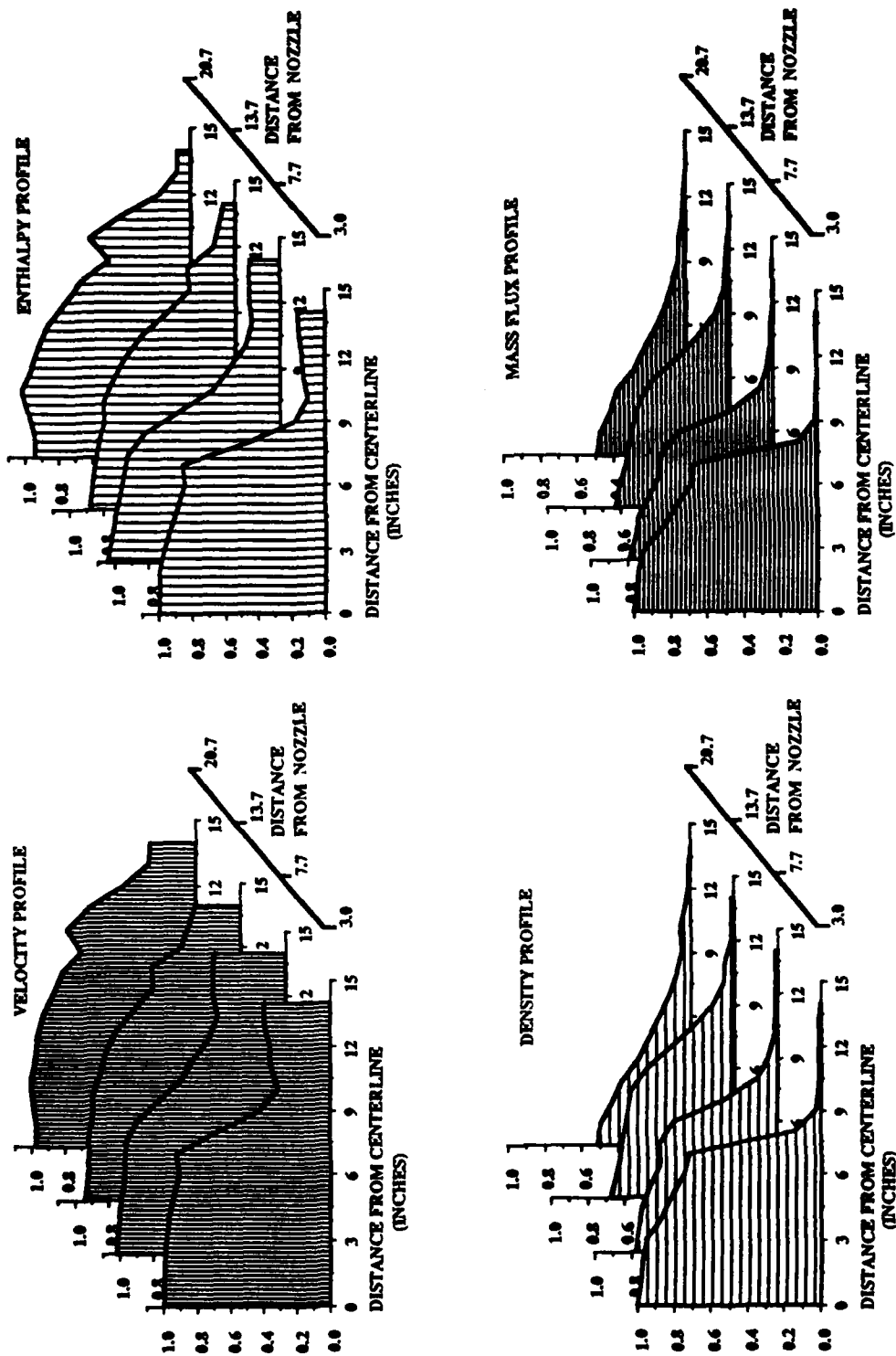
Figure 26   13-inch nozzle profiles normalized by 3-inch position from exit.
Constrictor conditions: 5000 Amps, 53 psia constrictor pressure, 18.5 MW arc power input.
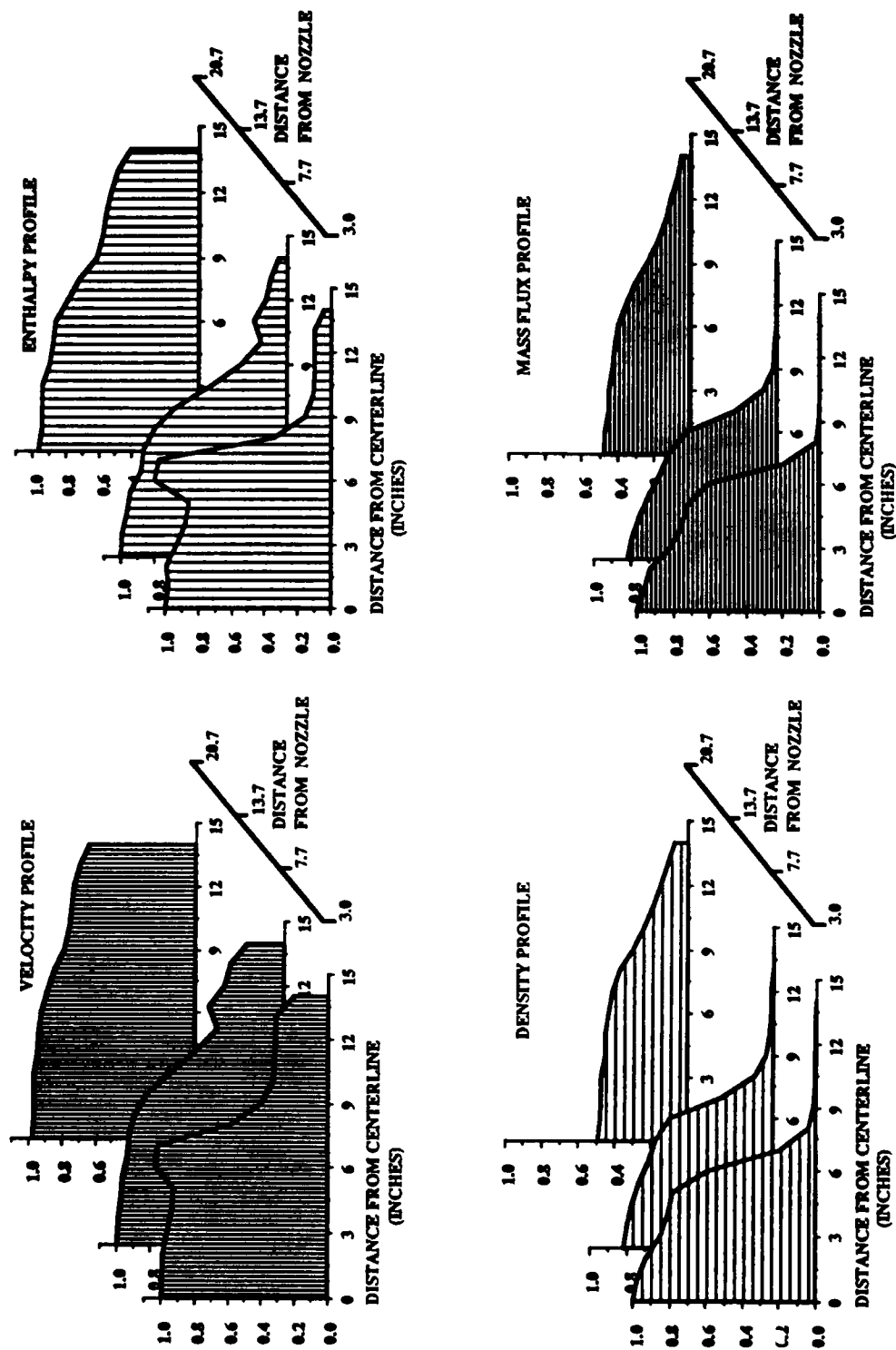
Figure 27   13-inch nozzle profiles normalized by 3-inch position from exit. Constrictor conditions: 5000 Amps, 78 psia constrictor pressure, 18.5 MW arc power input.
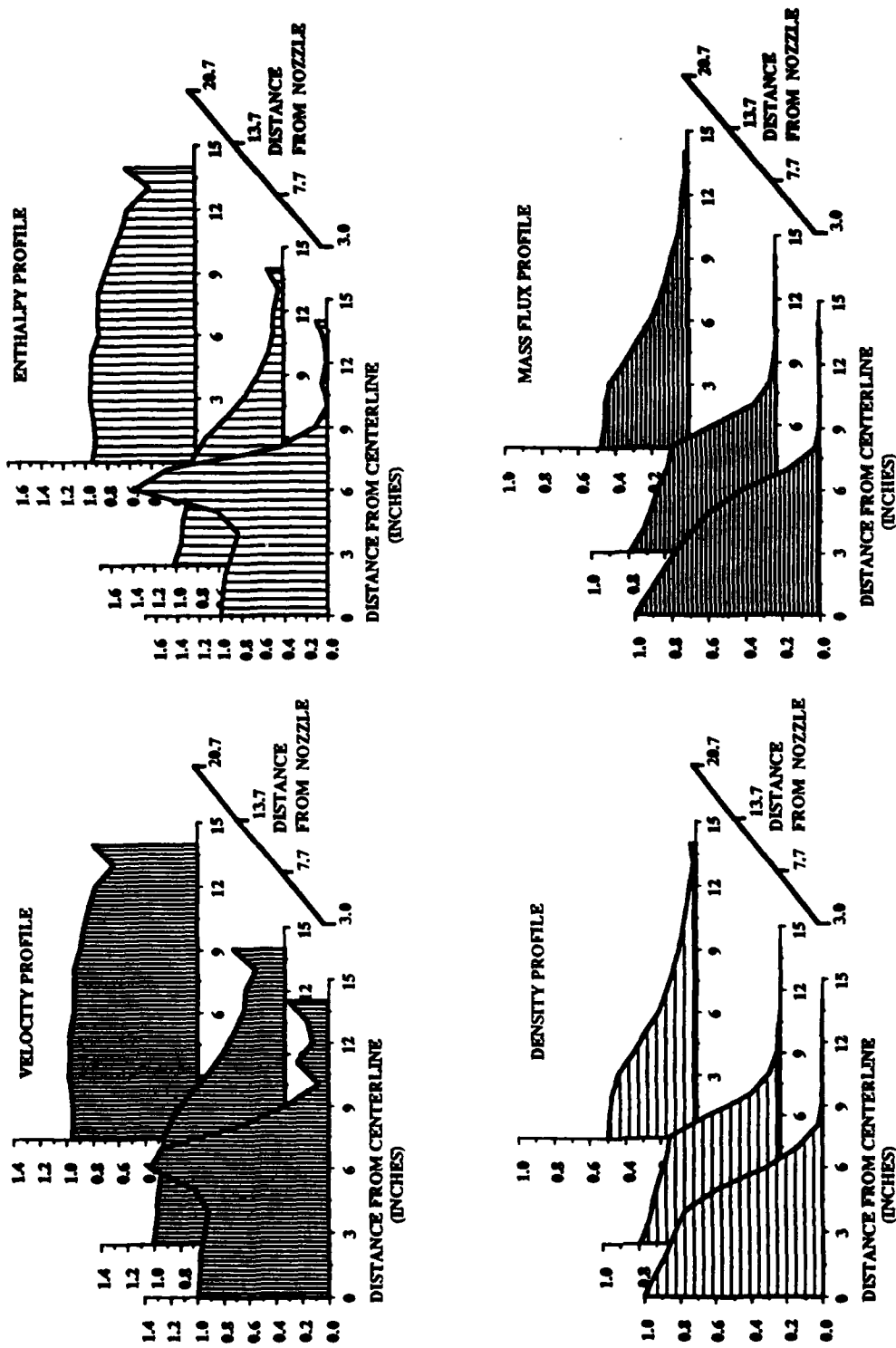
Figure 28 13-inch nozzle profiles normalized by 3-inch position from exit. Constrictor conditions: 6000 Amps, 109 psia constrictor pressure, 22 MW arc power input.

53

LIST OF REFERENCES

1. Winovich, W., Balboni, J. Balakrishnan, A.., "Application of Numerical Simulation to Enhance Arcjet Performance," AIAA Paper 85-1006, 1985, pp. 398-400.

2. Fay, J. A. and Riddell, F. R., "Theory of Stagnation Point Heat Transfer in Dissociated Air," _Journal of the Aeronautical Sciences_ , Vol. 25, 1958, pp. 73-85.

3. Stine, H. A.,,Watson,V. R., "The Theoretical Enthalpy Distribution of Air in Steady Flow Along the Axis of a Direct-Current Electric Arc," NASA TN D-1331,1962.

4. Nicolet, W. E. and others, "Analytical and Design Study for a High-Pressure, High-Enthalpy Constricted Arc Heater," AEDC TR-75-47, 1975.

INITIAL DISTRIBUTION LIST

No. Copies

1. Defense Technical Information Center 2
   Cameron Station
   Alexandria, Virginia 22304-6145

2. Library, Code 0142 2
   Naval Postgraduate School
   Monterey, California 93943-5002

3. Chairman, Code 67 1
   Department of Aeronautics and Astronautics
   Naval Postgraduate School
   Monterey, California 93943-5360

4. Prof. Richard Wood, Code 67Wr 2
   Naval Postgraduate School
   Monterey, California 93943-5360

5. Prof. Raymond Shreeve, Code 67Sf 1
   Naval Postgraduate School
   Monterey, California 93943-5360

6. Warren Winovich Code RTF 2
   NASA Ames Research Center
   Moffett Field, California 94035

7. John Balboni Code RTF 2
   NASA Ames Research Center
   Moffett Field, California 94035

8. Robert W. Kopp 3
   National Aero Space Plane
   AFSC/NAG
   Wright-Patterson AFB, Ohio 45433-6503

9. Howard Goldstein Code R   1
   NASA Ames Research Center
   Moffett Field, California 94035

10. Jim Arnold Code R   1
    NASA Ames Research Center
    Moffett Field, California 94035

11. Al Covington Code R   1
    NASA Ames Research Center
    Moffett Field, California 94035

12. Tom Polek   Code RTF   1
    NASA Ames Research Center
    Moffett Field, California 94035